La(III)-curcumin-functionallized gold nanocomposite as the red light-activable mitochondria-targeted PDT agent

Dulal Musib,[a] Vanitha Ramu,[b] Md Kausar Raza,[b] Aarti Upadhyay,[b] Maynak Pal,[a] Amit Kunwar[c], and Mithun Roy*[a]*

Supporting Information

Table of Content **Page no.**

Synthesis

Materials and Methods

Lanthanum(III) nitrate hexahydrate, curcumin, 1,10-phenanthroline-5-amine, lipoic acid, dicyclohexyl carbodiimide (DCC), $HAuCl_4.3H_2O$, tri-sodium citrate, Sephadex-25, MTT (3-(4,5-dimethylthiazol-2-yl)-2,5-diphenyltetrazolium bromide), DPBF (diphenylisobenzofuran), Rose Bengal (RB), Perylene, DCFDA (2',7'- dichlorofluorescin diacetate), Tetrabutylammonium perchlorate (TBAP**),** 3-(4,5-dimethylthiazol-2-yl)-2,5-

diphenyltetrazolium bromide (MTT), Caspases-3/7 and TEA were purchased from Sigma-Aldrich (USA). Other bio-chemicals or solvents were purchased from SD-Fine chemicals (India), HI-MEDIA, SRL Co., TCI Co., and were used as it was. The solvents used were purified as per the published protocols before use.[76]

UV–Visible and emission spectra were recorded on a Perkin-Elmer UV–Vis spectrometer and a HITACHI F-7000 fluorescence spectrophotometer, respectively. A Thermo Finnigan Flash EA 1112 CHNS analyzer was employed for elemental analysis. FT-IR spectra were recorded with a Perkin-Elmer UATR TWO FT-IR spectrometer using the KBr technique. EUTECH INSTRUMENT CON 510 (India) conductivity meter was used to determine the molar conductivity. ^{1}H NMR and ^{13}C NMR spectra were recorded on a Bruker Avance 400 (400 MHz) spectrometer, using $CDCl_3$ and DMSO-d_6 as solvents and tetramethylsilane (TMS) as an internal standard. The Q-TOF-ESI mass spectra were recorded with a Bruker Esquire 3000 Plus spectrometer (Bruker-Franzen Analytic GmbH, Bremen, Germany). High-performance liquid chromatography (HPLC) analyses were carried out with a Thermo fisher ultimate 3000 using daicel normal phase C18 column. The zeta potential was determined from Zetasizer Nano ZS90DLS zeta potential analyzer. TEM images were capture with an EDS apparatus-equipped high-resolution TEM. The absorbance readings of MTT assays were determined from Molecular Devices Versa Max tunable microplate reader. The flow cytometric assays as well as the confocal microscopy was carried out using a Becton Dickinson fluorescent-activated cell sorting (BD-FACS) Verse instrument (BD Biosciences) and Zeiss LSM 880 with Airyscan confocal microscope respectively. The confocal images were processed using Zeiss software. DFT and TD-DFT calculations were performed using the Gaussian 09 and material studio. The input files were prepared by using Gauss View 5.0.8.

Synthesis of 5-(1,2-dithiolan-3-yl)-N-(1,10-phenanthrolin-5-yl)pentanamide (L^1)

Lipoic acid (0.50 g, 2.42 mmol) in acetonitrile (CH_3CN) (5mL) and TEA (0.63 mL, 5 mmol) were mixed in a 100 mL round-bottom flask, followed by drop wise addition of DCC (1.26 g, 6.12 mmol). The reaction mixture was constant stirred under N_2 for 30 min at Room temperature. The 5-Amino-1,10- phenanthroline (0.48 g, 2.42 mmol) in CH_3CN (10 mL) was added to the reaction mixture and stirred at Room temperature under N_2 for 36 hr. Then the reaction mixture was worked up by ethyl acetate (30 mL) and H_2O (30 mL) to obtain a yellow solid. The yellow precipitate was washed with three times in 0.5N HCl (40mL) and saturated NaCl (10mL) and finally, dried over (Na_2SO_4). [yield: 0.76 g, 72%].

L^1: FT-IR solid phase: *ν*(C=N, C=O): 1513 cm^{-1}, 1730 cm^{-1}; HR-MS (m/z) in CH_3OH: m/z 384.1197 $(L^1H)^+$; ^{1}H NMR (DMSO-d_6, ppm, 400 MHz): δ 1.40-1.33 (m, 2H), 9.28- 9.27 (d, *J* = 4 Hz, 1H), 7.09-7.07 (d, *J* = 8 Hz, 1H), 8.83-8.79 (m, 1H), 8.24-8.22 (d, *J* = 8 Hz, 1H), 8.11-

8.02 (m, 2H), 7.95 (s, 1H), 7.09 (s, 1H), 3.62-3.58 (m, 2H), 3.18-3.12 (m, 2H), 2.42-2.37 (m, 1H), 2.28-2.24 (m, 2H), 1.89-1.80 (m, 2H), 1.58-1.53 (m, 2H). ^{13}C NMR (DMSO-d_6, ppm, 100 MHz): 26.37, 29.18, 32.63, 35.04, 50.44, 53.50, 56.97, 123.46, 125.68, 125.83, 131.14, 133.22, 134.31, 139.96, 139.41, 141.74, 146.73, 150.88, 154.52, 170.37.

Synthesis of AuNPs

A 50-ml aqueous solution of $HAuCl_4.3H_2O$ (2.5×10^{-4} M) was placed in a 250-ml round-bottom flask and stirred at 100˚C. After 15 min, 1.0 ml of 5% (0.17 M) aqueous trisodium citrate was added and stirred vigorously at the same temperature. After the solution was stirred for 25 min, its color changed gradually from transparent light yellow to dark black and finally to wine red, which is the characteristic color of colloidal AuNPs. The solution was then cooled to RT and purified by centrifugation. The AuNPs were characterized with reference to published characterization data.

AuNPs: Color: wine red. UV–Visible spectra in H_2O [λ_{max},/H_2O]: 520 nm; Powder XRD (2θ) : 38.22° (111 plane), 44.22°(200 plane), 64.72°(220 plane), and 77.69° (311 plane) [Au]. Avg. hydrated size in DLS spectra: 52 ± 5 nm. Zeta potential (ζ): −17.8 ± 5 mV.

Methods

1. Singlet oxygen ($^1O_2$) generation [1]

We have studied singlet oxygen ($^1O_2$) generation via UV-visible (UV-vis) spectrophotometry using 50 µM 1,3-diphenylisobenzofuran (DPBF). DPBF reacted with $^1O_2$ to form an endoperoxide, which decomposed to 1,2-dibenzoylbenzene. The UV-vis spectra of DPBF (λ_{max} 417 nm) were recorded in the presence of the complex (20 µM) and 1-AuNPs nano hybrid (100 µg/ml), exposed to visible light for 140 s. A gradual decrease in the absorbance of DPBF indicated the generation of $^1O_2$. We have measured decrease in absorbance of DPBF against the photo-exposure time to monitor the photoactivated generation of singlet oxygen.

2. Singlet oxygen ($^1O_2$) quantum yield determination [2]

Singlet oxygen quantum yield of the complex (1) and 1-AuNPs were determined in DMSO at ambient temperature. Visible light was used for the photo-sensitization of the complex (1), 1-AuNPs hybrid and Rose Bengal (RB). Quantum yields for singlet-oxygen ($^1O_2$), generate by the complex (1), 1-AuNPs

hybrid were determined by monitoring the photo-oxidation of DPBF. DPBF is a convenient acceptor because it absorbs in a region of dye-transparency and rapidly scavenges singlet oxygen to give colorless products. The quantum yields of singlet-oxygen generation were measured at low dye concentrations (optical density: 0.08– 0.12 at irradiation wavelengths 400-700 nm) to minimize the possibility of singlet-oxygen quenching by the dyes. The photo-oxidation of DPBF was monitored between 10 s to 140 s. The quantum yields of singlet oxygen generation ($\Phi[^1O_2]$) were calculated by a using relative method with optically matched solutions and by comparing the quantum yield of the photo-oxidation of DPBF that was sensitized by the compound of interest to the quantum yield of Rose Bengal (RB) ($\Phi[^1O_2]$= 0.76 in DMSO) as a reference compound according to equation (1),

$$\Phi\Delta_c = \Phi\Delta_{RB} \times (m_c/m_{RB}) \times (F_{RB}/F_c) \quad (1)$$

where c denotes a complex, and RB denotes Rose Bengal. $\Phi\Delta$ is the $^1O_2$ quantum yield, and m is the slope of the plot of DPBF absorbance at 417 nm vs. irradiation time. F is the absorption correction factor, which is given by Equation (2).

$$F = 1 - 10^{-OD}, \quad (2)$$

where OD is the optical density at the irradiation wavelength.

3. Computational details [3]

Theoretical calculations for the complex (1) was performed using Gaussian 09 version A.02 (Gaussian Inc., USA). The Gaussian 09 input files were prepared using Gauss View 5.0.8. The geometric structure, HOMO and LUMO of the complex in the ground state were fully optimized at the CAM-B3LYP/GEN level using 6-31G (d, p) basis sets for H, C, N, O, and S atoms. A LANL2DZ basis set was used for La atom in the gas phase.

Theoretical calculations of AuNPs and 1-AuNPs was done using material studio software.

4. MTT assay [4]

The 3-(4,5-dimethylthiazol-2-yl)-2,5-diphenyltetrazolium bromide (MTT) assay was used for the photocytotoxicity of the 1-AuNPs hybrid and complex (1). In this assay, the mitochondrial dehydrogenases of viable cells cleaved the tetrazolium rings of MTT forming dark purple insoluble formazan crystals that were soluble in DMSO and was quantified from spectral measurements. Approximately, 2500-5000 cells was plated separately in two different 96 wells culture plate and incubated with various concentrations of 1-AuNPs and complex 1 from 5 to 400 µg/ml 3.2 to 100 µM in 1% DMSO/Dulbecco's modified Eagle's medium (DMEM) for 4 h in the dark. After 4 h of incubation, the media containing compounds was removed and replaced with DPBS buffer for one set of the cells which were exposed to red light (λ = 600-720 nm, light dose = 30 J cm^{-2}), using Waldmann

PDT 1200 L, whereas the other set was kept in the dark for the same time period using standard protocols. After exposure to light, DPBS was removed and replaced with fresh medium and incubation was continued for a further period of 19 h 20 min in dark for the plate thus making the total incubation time of ~21 h. After the incubation period, 5 mg mL-1 of MTT (20 μL) was added to each well and incubated for an additional 3 h. The media was removed entirely from the wells and then DMSO (200 μL) was added and spectral measurement was taken at 570 nm using TECAN microplate reader. Cytotoxicity of the 1-AuNPs and complex were measured as the percentage ratio of the absorbance of the treated cells to the untreated controls. The IC_{50} values were determined by nonlinear regression analysis (Graph Pad Prism 6). Data were obtained by using three independent sets of experiments done in triplicate for each concentration.

5. Cellular Localization [5]

By using confocal microscopy, the intracellular localization of the green fluorescent complex (1) and 1-AuNPs (5 μM and 13 μg/ml) in 1% DMSO/DMEM was investigated by confocal microscopy (Zeiss LSM 880 with Airyscan) using an oil immersion lens having a magnification of 63X. About 5 x 10^4 A549 cells were plated on glass cover slips in 12 well tissue culture plates and incubated at 37°C and 5% CO_2 atmosphere for 24 h. Cells were then treated with the complex (1) and 1-AuNPs for 4 h in dark and fixed. Cells were later incubated with DAPI (1 mg/mL) for 5 min to stain the nucleus and Mitotracker® red (MTR, 0.1 μM) to stain the mitochondria. The cover slips were subjected to confocal microscopy after being mounted on slides. Multiple images were recorded, and experiments were done in duplicates to confirm the results.

6. ROS generation [6]

Cellular reactive oxygen species (ROS) was detected by 7'-dichlorofluorescein diacetate (DCFDA) assay and Singlet Oxygen Sensor Green (SOSG). Cellular ROS oxidizes cell permeable DCFDA generating a fluorescent DCF having emission maxima at 528 nm. On the other hand, SOSG is a weakly blue fluorescent probe that shifts its emission to the green region in the presence of singlet oxygen inside the cell. The percentage population of cells generating ROS was determined by flow cytometry analysis. A549 cells were incubated with the 1-AuNPs and complex at their IC_{50} values [1-AuNPs (13 μg/ml) and complex (5 μM)] for 4 h and then irradiated with red light for 40 min (λ = 600-720 nm, light dose = 30 J cm^{-2}) using Waldmann PDT 1200 L. The cells were harvested by trypsinization and a single cell suspension was prepared. The cells were subsequently treated with 1 μM DCFDA or SOSG (solution prepared with DMSO) in dark for 20 min at room temperature. The distribution of DCFDA stained A549 cells was obtained by flow cytometry in the FL-1 channel. Additionally, the cellular hydrogen peroxide and superoxide levels were detected by staining cells with

5 μM of dihydrorhodamine123 (DHR123) and dihydroethidium (DHE) respectively for 30 min and monitoring the fluorescence through multiwall plate reader.

7. Cellular Uptake Mechanism Studies by Confocal Microscopy [7]

A549 cells (about 5 x 10^4) were plated on glass cover slips in 12 well tissue culture plates and incubated at 37°C and 5% CO_2 atmosphere for 24 h. Then the cells were incubated with 1-AuNPs (13 μg/ml) and complex (5 μM) at 4 and 37°C for 4 h. For confocal microscopy analysis, the cells were then washed three times with PBS and visualized by confocal microscopy (Zeiss LSM 880 with Airyscan) with an oil immersion lens having a magnification of 63X.

8. Annexin-V- FITC/Propidium iodide (PI) assay [9]

About 3 x 10^4 cells were plated in 6 well plates and grown for 24 h. Cells were treated with both the 1-AuNPs and complex (1) for 4 h. One of the plates was exposed to photo-irradiation (600-720 nm, 1 h) in DPBS with subsequent addition of fresh media. The cells were further incubated for 1 h, trypsinized and washed in DPBS twice. The cells were resuspended in 400 μL of 1X binding buffer and 1 μL of annexin V-FITC and 2 μL of PI were added to each cell suspension. These tubes were then incubated at room temperature for 20 min in dark. The fluorescence of the cells was measured immediately with a flow cytometer. Cells that are early in the apoptotic process were stained with the annexin VFITC alone. Live cells showed no staining by either PI or annexin V-FITC. Late apoptotic cells were stained by both PI and annexin V-FITC. The dead cells were only stained by PI. A549 cells were plated in 6-well culture plates for Propidium Iodide (PI) based cell cycle analysis. The cells were treated 1-AuNPs and complex (13 μg/ml and 5 μM, 4 h incubation) with or without 1 h of photo-irradiation (600-720 nm). After 12- 15 hours, the monolayer cultures were used for the analysis. The media was removed and cells were washed with PBS. Hypotonic PI citrate stain (50 μg/mL PI in 0.10% trisodium citrate dihydride containing 0.10% Triton X-100) was added to the monolayer and cells were scraped with a rubber policeman. The cell suspension was taken into an eppendorf and centrifuged at 800 rcf, 4 °C for 7 min. The nuclear pellet was resuspended in fresh hypotonic PI citrate stain and was used for FACS analysis.

9. Cellular uptake studies in WI-38 cells

In brief, cells (2×10^3 per well) seeded in a 96-well microplate were treated with complex **1** (12 μM) and **1**-AuNPs (12 μg/mL) in a total volume of 200 μl for 4 hours at 37 °C in a humidified incubator with 5% CO_2 atmosphere. Following this, cells were washed thrice with room temperature phosphate

buffered saline (PBS), resuspended into 200 µl of PBS and subjected to fluorescence measurement at 557 nm using multi well plate reader (Synergy H1, BioTek, USA) after excitation at 450 nm.

10. Protein expression analysis

The expression levels of BAX, Bcl-2 and cleaved caspase-3 were examined by intracellular antibody staining followed by flow cytometry analysis as described previously [1]. The fold changes were calculated by normalizing mean fluorescence intensity (MFI) of viable cell population (hoechst 33342 positive) of treatment group to that of control using FlowJo® software after acquiring on flow cytometer (Partec, Germany). For each experiment, a minimum of 10000 events per sample were recorded.

11. Calculating the concentration of gold nanoparticles (AuNPs) and complex (1) coverage on gold nanoparticles (AuNPs)

Mass of HAuCl4 (49 % Au by assay) = 0.01257
Mass (Au) = 0.49 x 0.01257 = 0.006159 g
moles (Au) = 0.006159 / 197 = 3.229 x 10-6 moles
[Au] = 3.229 x 10^{-6} moles / 0.120 dm3 = 2.691 x 10-5 M.
Number of Au atoms per 15 nm nanoparticle = 4/3 x 3.14 x (7.5 x 10-9) 3 / (0.417) 3 = 24301 (assuming that the particles are spherical and estimated atomic radius of gold = 0.417nm).
Concentration of AuNP15 = 2.691 x 10-5M / 24301 = 1.1 nM.
The coverage of complex (1) in 1-AuNPs hybrid.
ICPOES results give an La : Au atomic ratio of 1:64.
From the calculation of the number of Au atoms per 15 nm particle, 24301Au atoms per nanoparticle are estimated which leads to 24301/64 = 380 of complex (1) per nanoparticle.

12. Octanol/water partition coefficient (log Po/w)

The partition-coefficient of 1-AuNPs hybrid, expressed as

log Po/w = log {[solute]octanol/[solute]water}

can be determined by “shake-flask” method. 1-AuNPs mixed with Water and octanol mixture and shook thoroughly upto 24 h. to reach equilibrium, which results in separation of two layers. The concentration

of nano hybrid was determined by UV-Visible spectroscopy using the extinction coefficients of the hybrid in water saturated with octanol.

References

1. Musib, D.; Banerjee, S.; Garai, A.; Soraisam, U.; Roy. M. Synthesis, Theory and In Vitro Photodynamic Activities of New Copper (II)-Histidinito Complexes. *Chemistry Select.* **2018**, *3*, 2767-2775.

2. Raza, K.; Gautam, S.; Garai, A.; Mitra, K.; Kondaiah, P.; Chakravarty, A. R. Monofunctional BODIPY-Appended Imidazoplatin for Cellular Imaging and Mitochondria-Targeted Photocytotoxicity. *Inorg. Chem.* **2017**, *56*, 11019-11029.

3. Barolo, C.; Nazeeruddin, M. K.; Fantacci, S.; Censo, D. D.; Comte, P.; Liska, P.; Viscardi, G.; Quagliotto, P.; Angelis, F. D.; Ito, S.; Grätzel. M.Synthesis, Characterization, and DFT-TDDFT Computational Study of a Ruthenium Complex Containing a Functionalized Tetradentate Ligand.*Inorg. Chem.* **2006**, *45*, 4642–4653.

4. Elmes, R. B. P.; Orange, K. N.; Cloonan, S. M.; D. C. Williams, D. C.; Gunnlaugsson, T. Luminescent Ruthenium(II) Polypyridyl Functionalized Gold Nanoparticles; Their DNA Binding Abilities and Application As Cellular Imaging Agents.*J. Am. Chem. Soc.* **2011**, *133*, 15862–15865.

5. Chanu, S. B.; M. K. Raza, M.K.; Banerjee, S.; Mina, P. R.; Musib, D.; Roy, M. ROS dependent antitumour activity of photo-activated iron (III) complexes of amino acids. *J. Chem. Sci.* **2019**, *131*, 9.

6. Zhou, Z.; Liu, J.; Rees, T. W.; Wang, H.; Li, X.; Chao, H.; Stang, P. J. Heterometallic Ru-Pt metallacycle for two-photon photodynamic therapy.*Proc Natl Acad Sci U S A.* **2018**, *115*, 5664-5669.

7. Rogers, J. N.; Claire, S.; M. Harris, R.; Farabi, S.; Zikeli, G.; Styles, I. B.; Hodges, J. N.; Pikramenou, Z. High coating of Ru(II) complexes on gold nanoparticles for single particle luminescence imaging in cells. *Chem. Commun*. **2014**, *50*, 617-619.

8. Skehan, P.; Storeng, R.; Scudiero, D.; Monks, A.;McMahon, J.; Vistica, D.; Warren, T. J.; Bokesch, H.; Kenney, S.; Boyd, R. M. New colorimetric cytotoxicity assay for anticancer-drug screening. *J. Natl. Cancer Inst*. **1990**, *82*, 1107-1112

9. Bechet, D.; Couleaud, P.; Frochot, C.; Viriot, M.-L.; Guillemin, F.; Barberi-Heyob, M. Nanoparticles as Vehicles for Delivery of Photodynamic Therapy Agents. *Trends Biotechnol.* **2008**, 26, 612.

Table S1. Selected Physicochemical data of the Ligand (**L^1**), **1** and **1-AuNPs**.

Ligand (**L^1**) and complex (**1**)	**L^1**	**1**	**1-AuNPs**
IR[a]: υ/cm^{-1}	1730,1537 (C=O, C=N)	3250, 1651,1523 (OH, C=O, C=N)	3344, 1602, 1528 (OH, C=O, C=N)
Λ_M[b]: /Ω^{-1} cm^2 mol^{-1}	-	32	-
Q-TOF ESI MS (m/z)[c]	384.1197 $(L^1H)^+$	1256.2690 $[M-(NO_3^-)]^+$ and 951.4533 $[M-(HCur)]^+$.	-
Electronic[d]: MLCT/LMCT/ λ_{max} / nm (ε × 10^{-4}/L mol^{-1} cm^{-1} for 1 and absorbance for 1-AuNPs))	-	496 sh (0.011), 450 (1.64), 426 (1.86)	755 (1.01) (SPR), 539 (1.22), 424 (1.65)
λ_{em}/ nm[e] [λ_{ex}= 350 nm (L^1), 450nm (1, AuNPs)]	564	557	486, 553
Φ ($^1O_2$) (20 µM for 1, 100 µg/ml for 1-AuNPs) [f]	-	0.55	0.69
$E_{1/2}$(V)[g] (1mM for 1 and 100 µg/ml for 1-AuNps) [g]	-	-0.44	-0.51

[a]Infrared data for ligand (**L^1**), **1 and 1-AuNPs**;[b]Molar conductivity data of the complex in 5 % DMSO-H_2O at 25 ºC; [c]Q-TOF ESI Mass spectra of the complex recorded in CH_3OH; [d]UV-visible spectra of the complex in 5 % DMSO-H_2O and 1-AuNPs in H_2O at 25 °C; [e]Luminescence spectra of the ligand (L^1), complex (1) recorded in 5 % DMSO-H_2O and 1-AuNPs in H_2O 25 °C; [f] Singlet oxygen quantum yield of the complex (1) and 1-AuNPs, RB is a standard; [g] $E_{1/2}$ value of the complex and 1-AuNPs in DMF.

Table S2: Calculated h,k and l value from Powder XRD data.

line	position(2θ)	theta(radians)	Sinθ	Sin^2(θ)	Ratio 1	Ratio 2	Ratio 8	m	hkl
21.35	10.675	0.1852	0.1852	0.034	1	2	8	8	220
23.48	11.742	0.2035	0.2035	0.041	1.207	2.41	9.65	10	310
24.71	12.357	0.214	0.214	0.045	1.334	2.66	10.67	11	311
25.69	12.849	0.2223	0.2223	0.049	1.4412	2.88	11.53	12	222
38.34	17.625	0.3283	0.3283	1	2	3	3	3	111
44.51	11.625	0.3787	0.3787	1.33	2.6604	3.99	3.99	4	200
64.58	11.75	0.5342	0.5342	2.64	5.2931	7.93	7.93	8	220
77.96	11.75	0.6290	0.6290	3.66	7.3395	11.0	11.0	11	331

Table S3: The stability study of AuNPs and 1-AuNPs by DLS instrument.

Temperature (days)	Sample	Size (nm)	Zeta potential (mV)
25˚C (0 day)	AuNPs	52 ± 5	-17.8 ± 5
25˚C (1 day)	AuNPs	54 ± 5	-17.6 ± 5
25˚C (5 days)	AuNPs	59 ± 5	-17.0 ± 5
25˚C (15 days)	AuNPs	61 ± 5	-17.3 ± 5
25˚C (30 days)	AuNPs	65 ± 5	-16.9 ± 5
25˚C (0 day)	1-AuNPs	91 ± 12	-10.5 ± 5
25˚C (1 day)	1-AuNPs	93 ± 12	-10.1 ± 5
25˚C (5 days)	1-AuNPs	99 ± 12	-9.9 ± 5
25˚C (15 days)	1-AuNPs	109 ± 12	-9.6 ± 5
25˚C (30 days)	1-AuNPs	121 ± 10	-9.7 ± 5
4˚C (60 days)	1-AuNPs	101 ± 11	-9.9 ± 5
4˚C (90 days)	1-AuNPs	104 ± 10	-9.7 ± 5

Table S4: Photo-toxicity data (IC_{50}/µM) of the Lanthanium complex (1) and 1-AuNPs in A549, and HaCaT cells by CVS assay.

	A549 cells		HaCat Cells	
	Dark	Red light	Dark	Red light
1	>100	17.2 ± 1.8	>100	21.1 ± 2.1
1-AuNPs	>500	34 ± 3 µg/mL	>500	42 ± 2 µg/mL

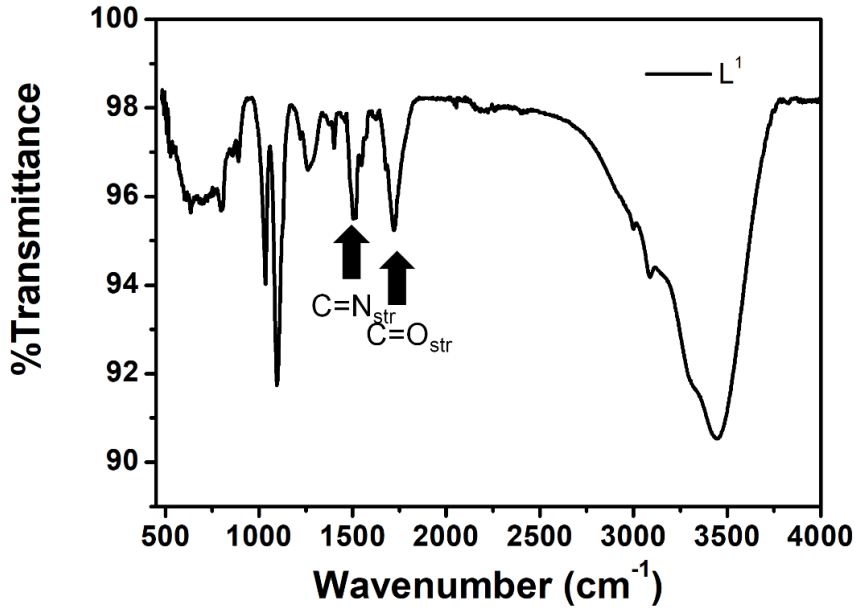

Figure S1: FT-IR Spectra of **L[1]** recorded in KBr phase using Perkin-Elmer UATR TWO FT-IR Spectrometer.

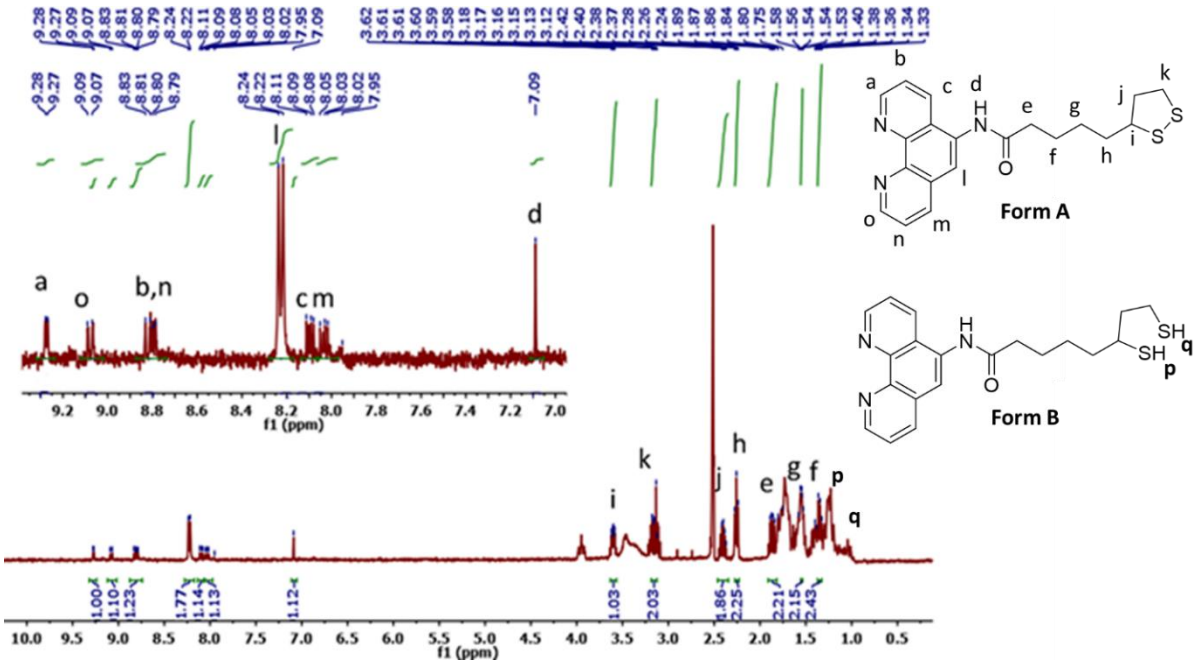

Figure S2: ^{1}H NMR of **L[1]** recorded in DMSO-d_6 using Bruker Avance 400 (400 MHz) spectrometer. Typically, the disulphide bond of **L[1]** is reduced to an open form (form B), that gives rise to additional peaks in the range of 1.25-1.0 ppm in the ^{1}H NMR spectra (Wada, N.; Wakami, H.; Konishi, T.; Matsugo, S.; The Degradation and Regeneration of α-Lipoic Acid under the Irradiation of UV Light in the Existence of Homocysteine, *J. Clin. Biochem. Nutr.* **2009**, 44, 218-222.)

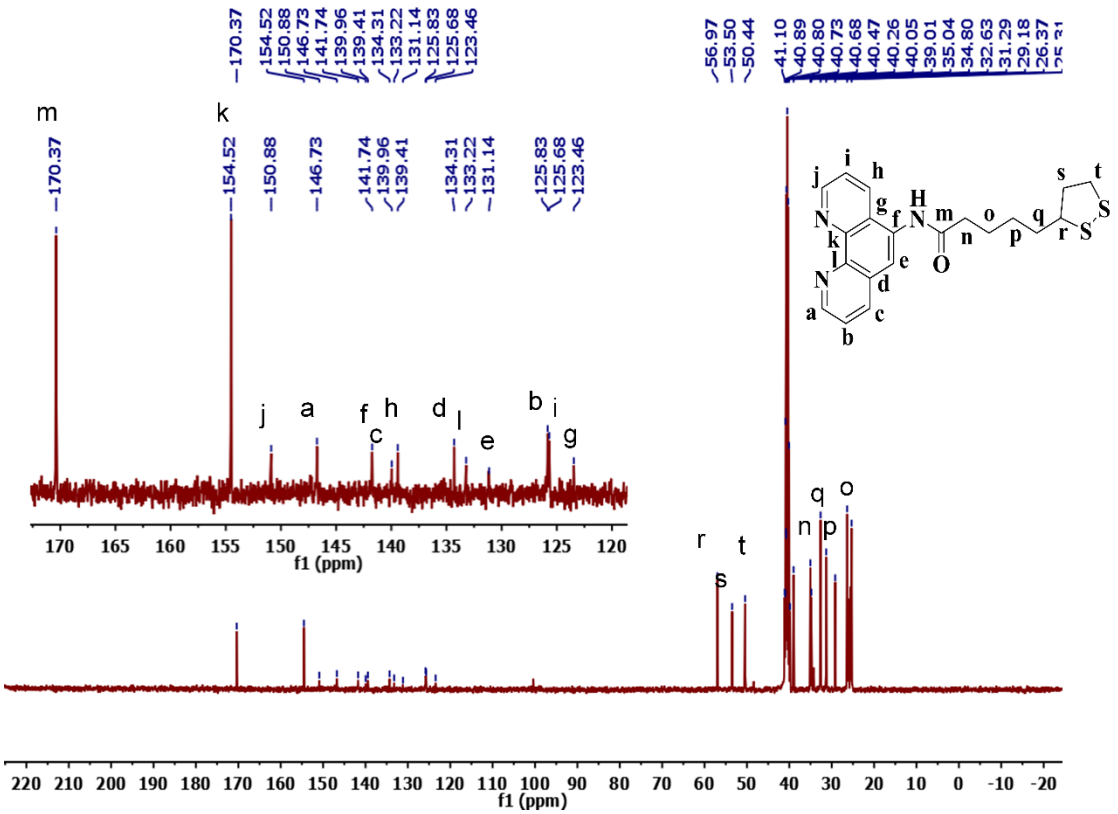

Figure S3: ^{13}C NMR of **L^1** recorded in DMSO-d$_6$ using Bruker Avance 400 (100 MHz) spectrometer.

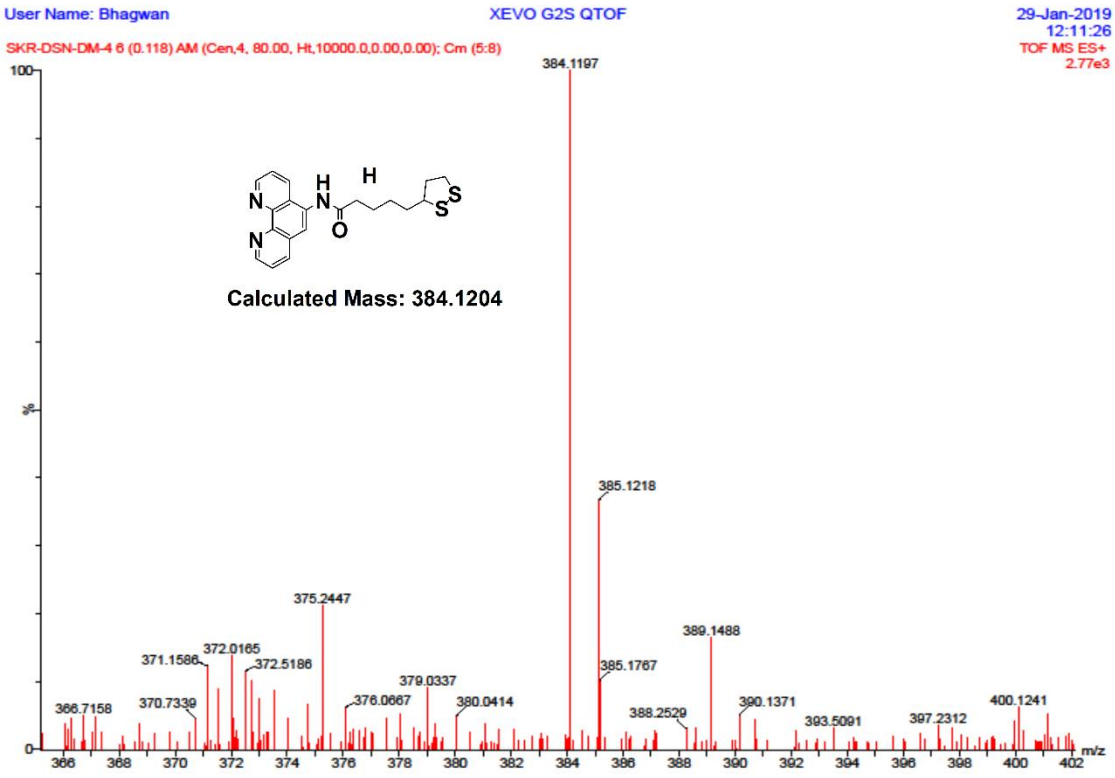

Figure S4: HR-Mass spectra of the **L^1** recorded in CH_3OH. The peak at m/z 384.1197 corresponds to the species [**L^{1}H**]$^+$.

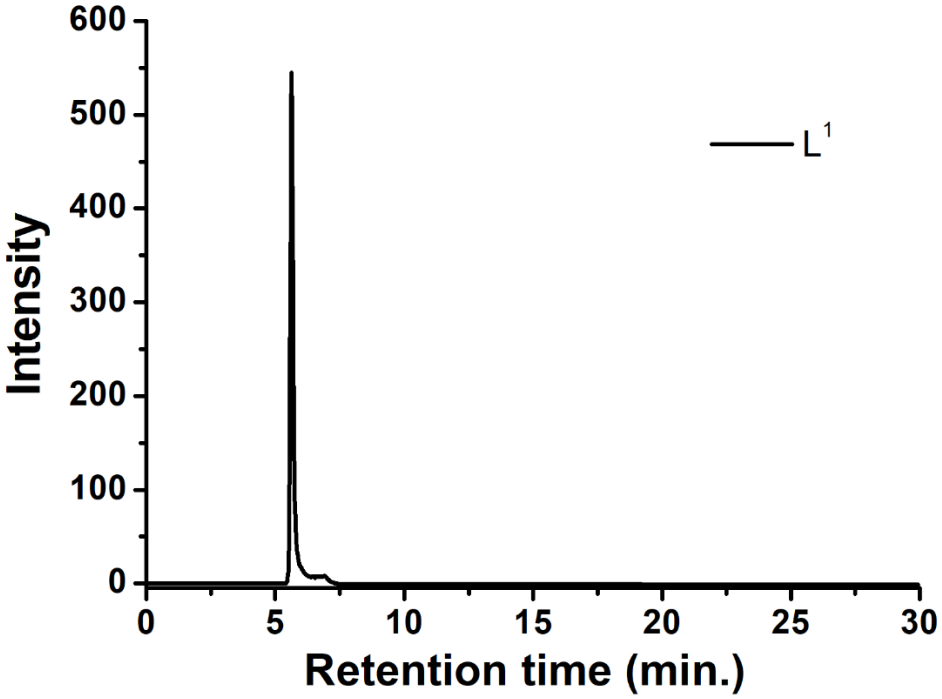

Figure S5: HPLC chromatograms for the ligand (**L^1**) **(**Condition: UV = 254nm, flow rate 0.5 ml/min, solvent = H_2O: CH_3OH = 90:10).

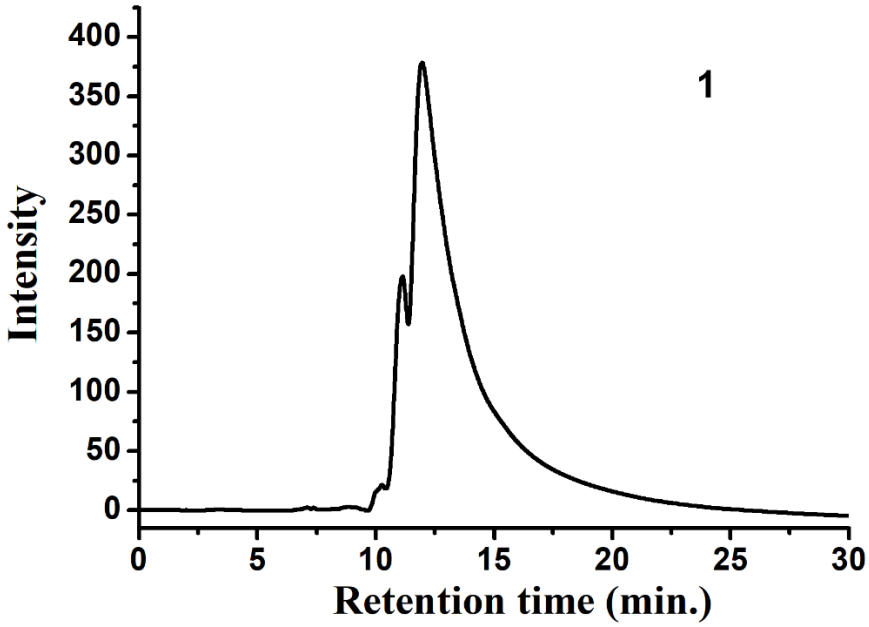

Figure S6: HPLC chromatograms for the complex (1) **(**Condition: UV = 254nm, flow rate 0.5 ml/min, solvent = H_2O: CH_3OH = 80:20).

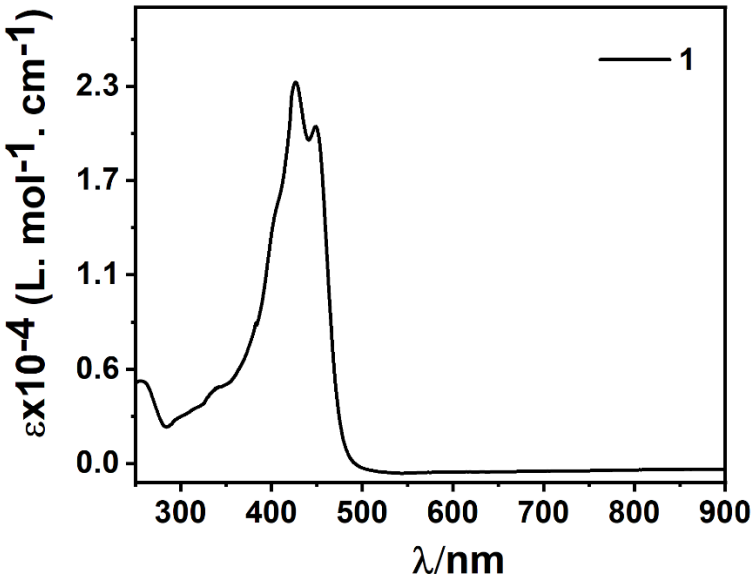

Figure S7: UV-Visible spectra of the complex (**1**) in 2% DMSO-H_2O in DMEM cell media.

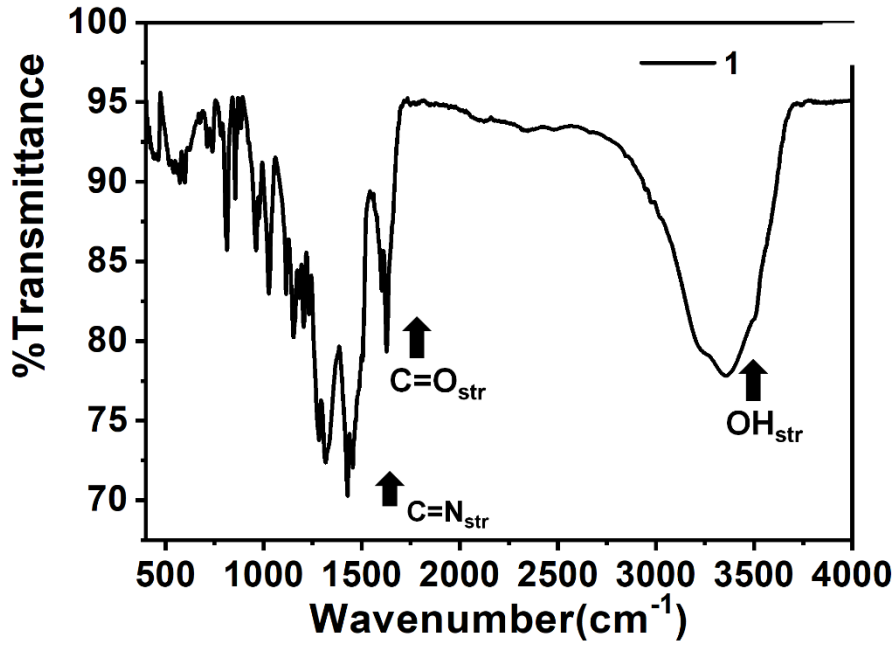

Figure S8: Solid phase FT-IR spectra of the complex 1.

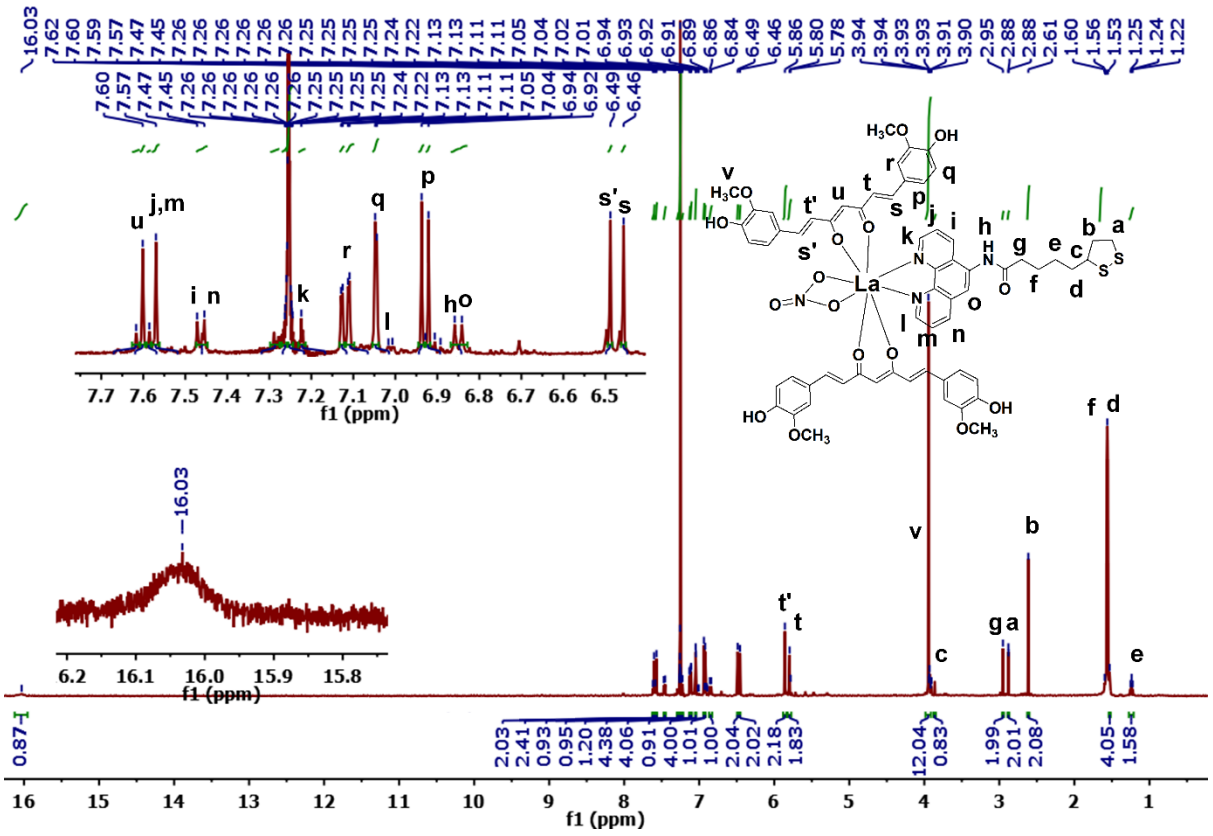

Figure S9: ^{1}H NMR of **1** recorded in DMSO-d_6 using Bruker Avance 400 (400 MHz) spectrometer.

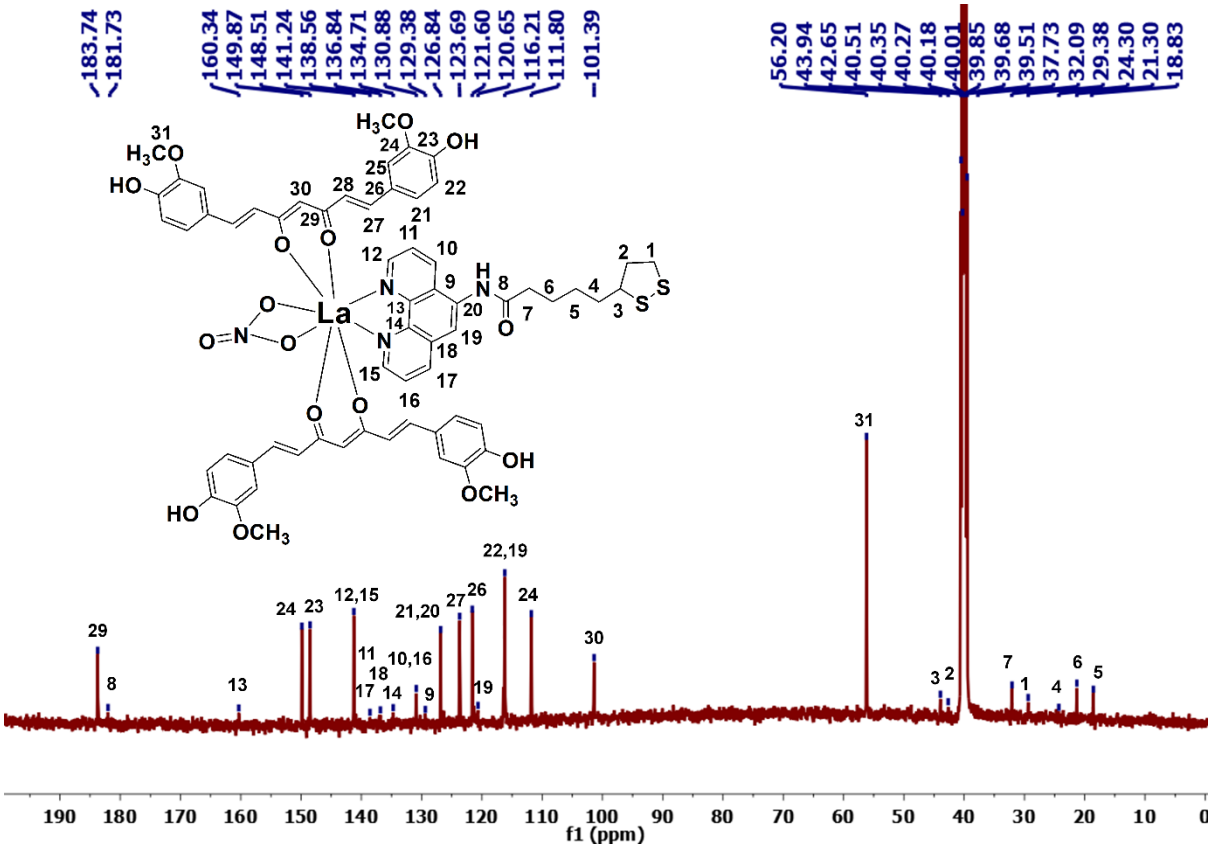

Figure S10: ^{13}C NMR of **1** recorded in DMSO-d_6 Bruker Avance 400 (100 MHz) spectrometer.

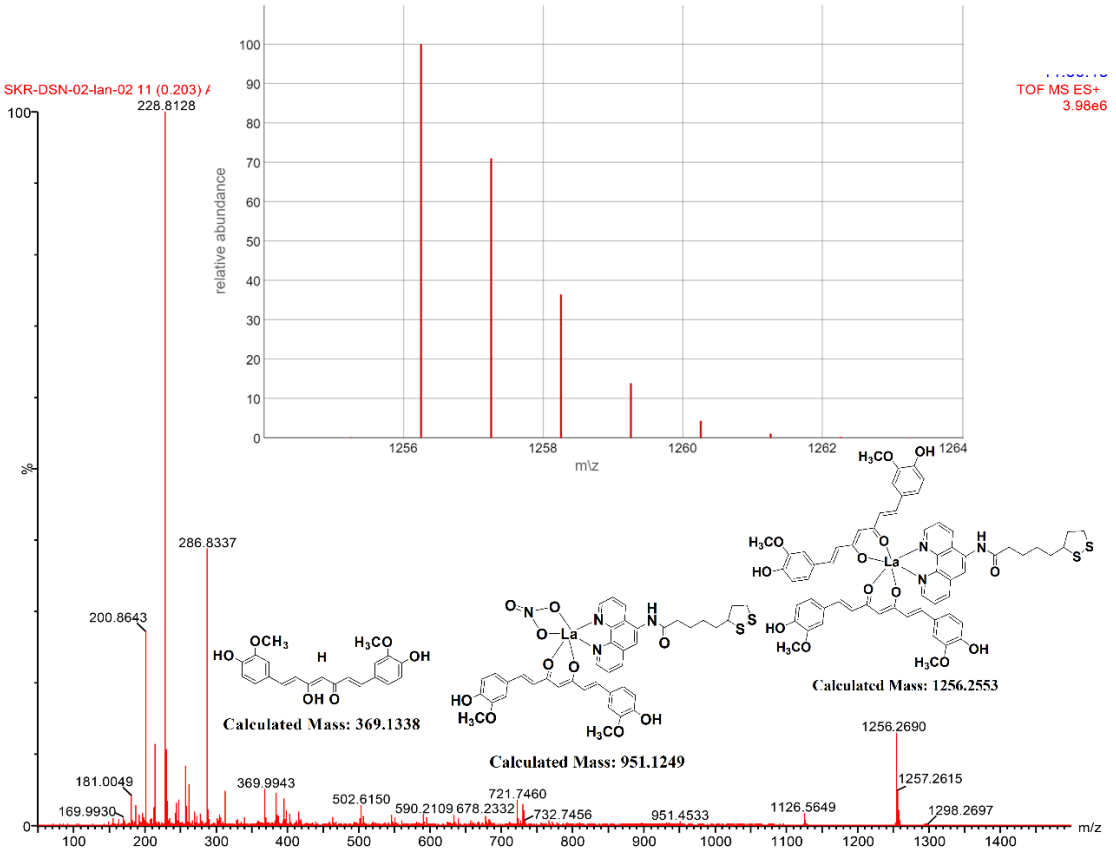

Figure S11: Q-TOF ESI Mass spectra of the **1** recorded in CH_3OH using Bruker Esquire 3000 Plus spectro-photometer (Bruker-Franzen Analytic GmbH, Bremen, Germany). The peak at m/z 1256.2690 corresponds to the species $[M-(NO_3^-)]^+$ and the highest peak 951.4533 corresponds to the species $[M-(Cur)]^+$.

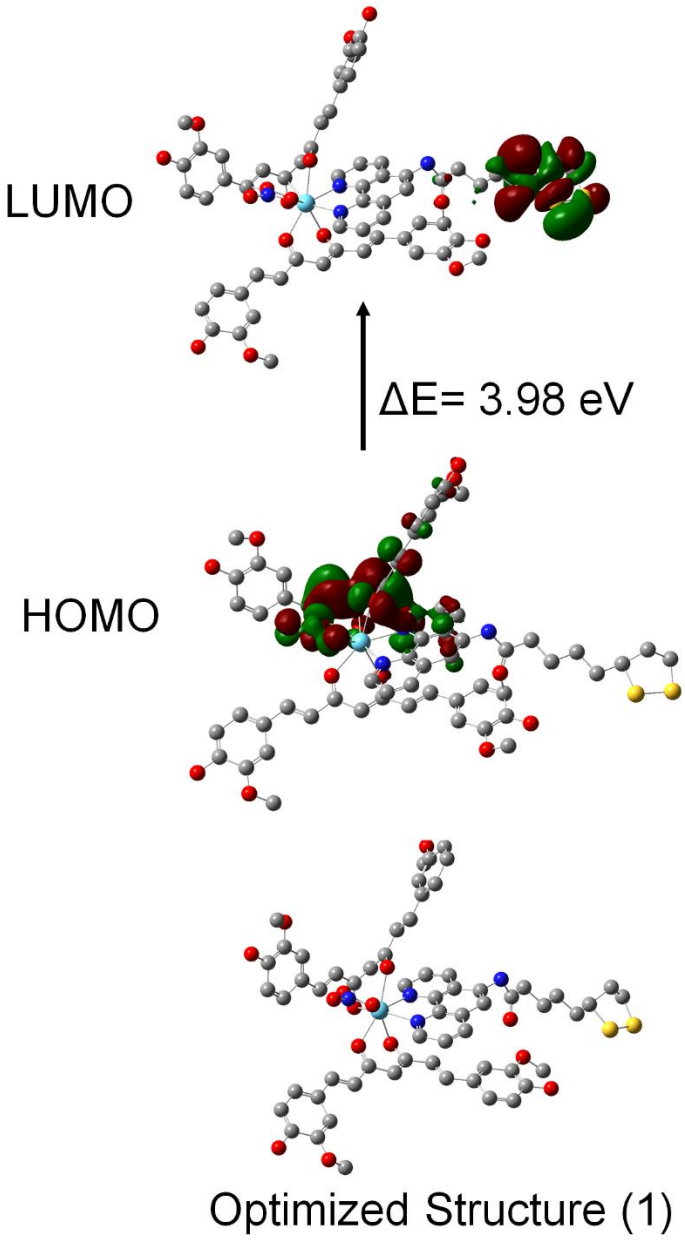

Figure S12: Optimized structure, HOMO and LUMO stereographs of the complex from DFT calculation at DFT/CAM-B3LYP/6-31G(d)/LanL2DZ level using Gaussian 09W software.

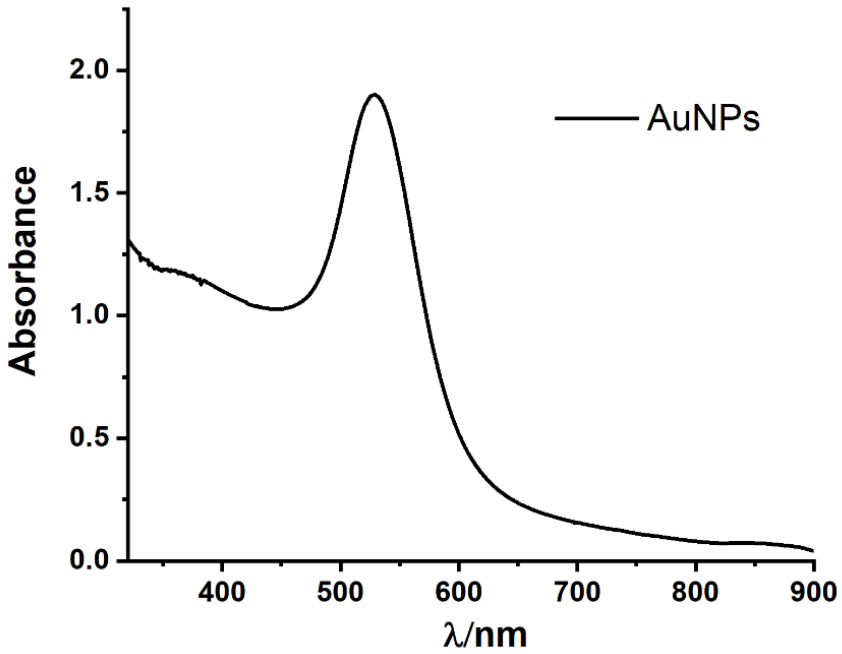

Figure S13: UV-Visible spectra of the AuNPs in double distilled water at pH 7.2**.**

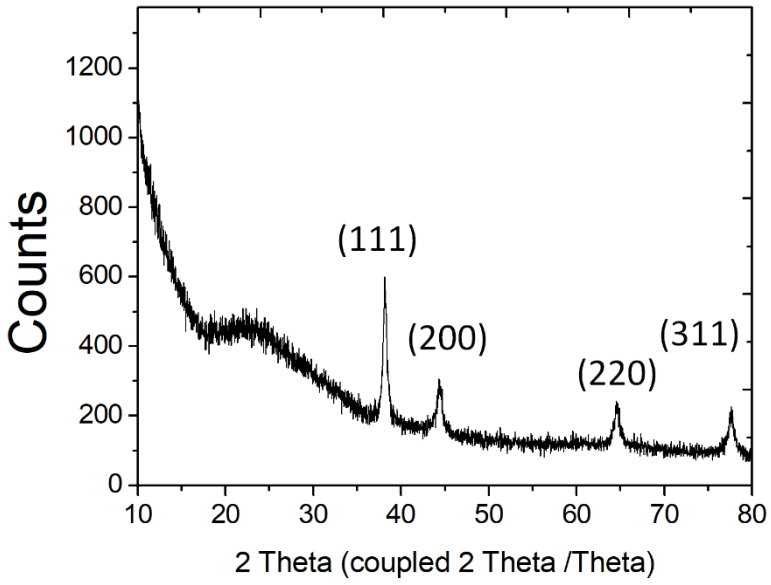

Figure S14: Powder XRD spectra of Gold-nanoparticles (**AuNPs**).

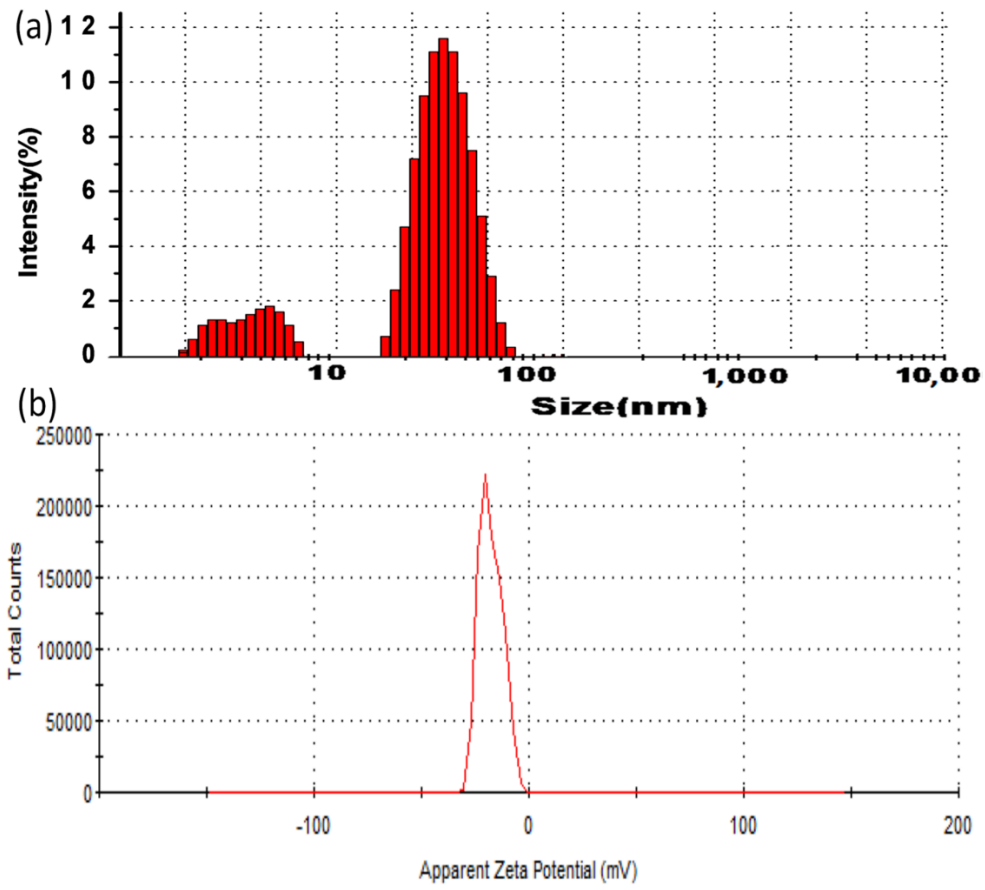

Figure S15: (a) Distribution of the size of the Gold-nanoparticles (**AuNPs**) determined by using DLS spectrometer. (b) Zeta potential graph of Gold-nanoparticles (**AuNPs**) determined from DLS measurements.

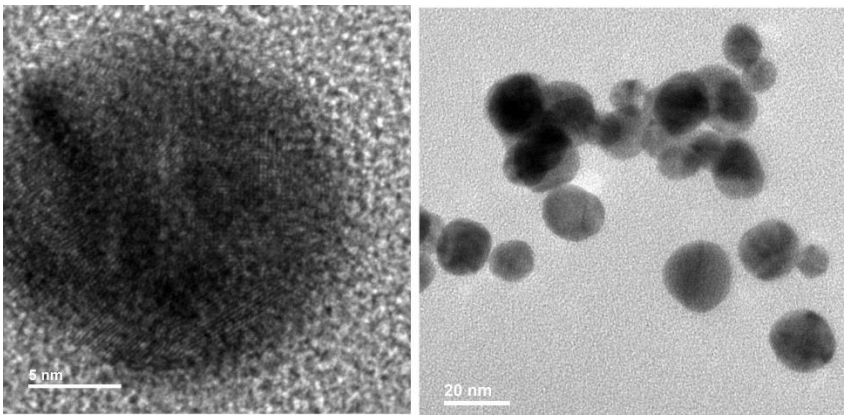

Figure S16: TEM image of **1-AuNPs** hybrid.

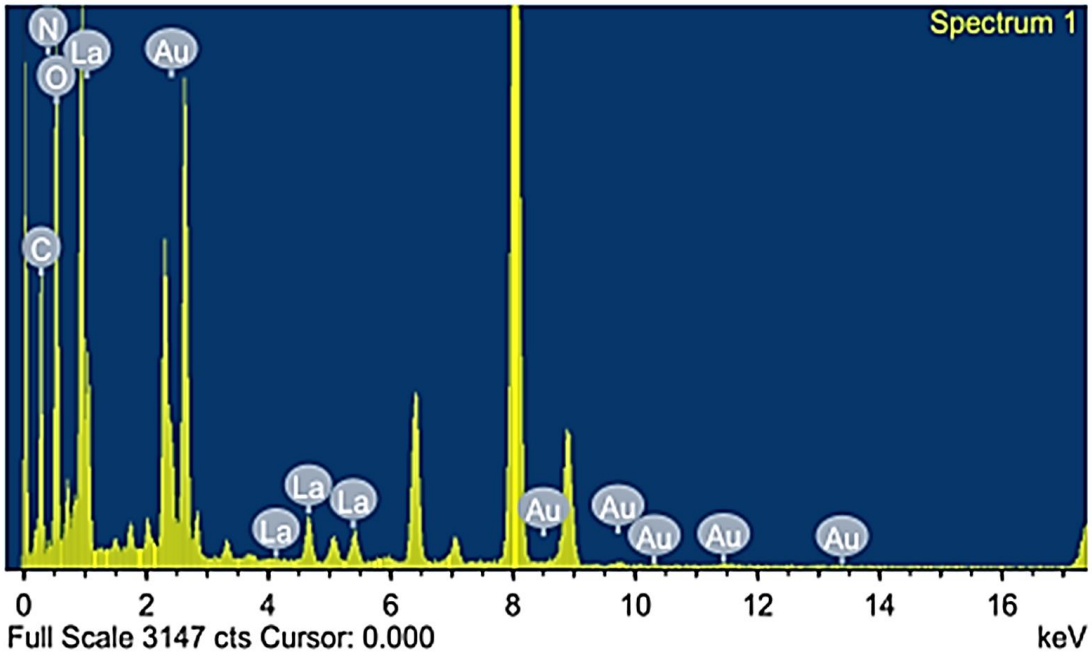

Figure S17: EDX spectrum of the **1-AuNPs** hybrid.

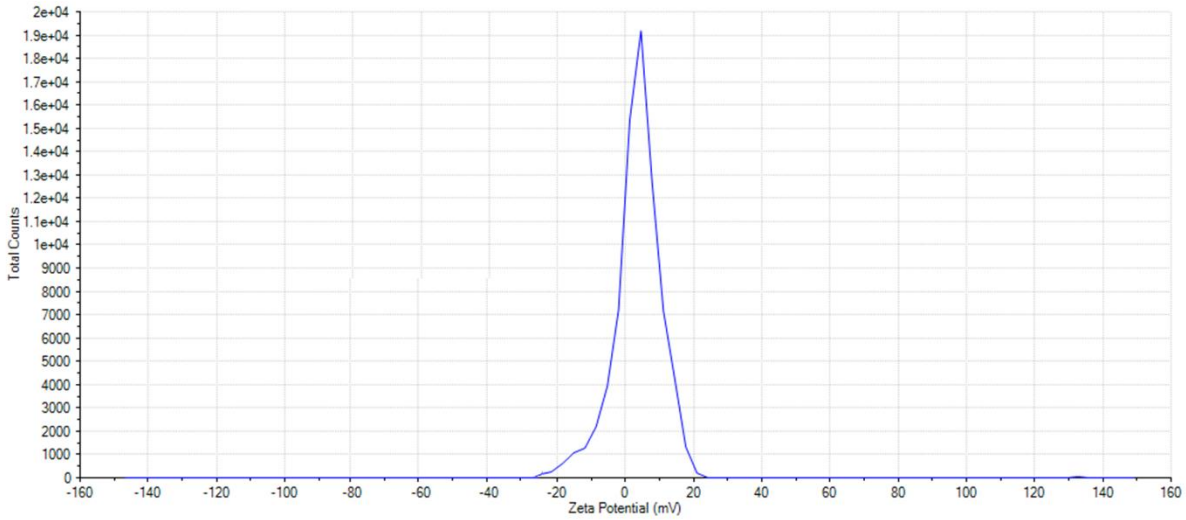

Figure S18: Zeta potential graph of **1-AuNPs** hybrid determined from DLS measurements.

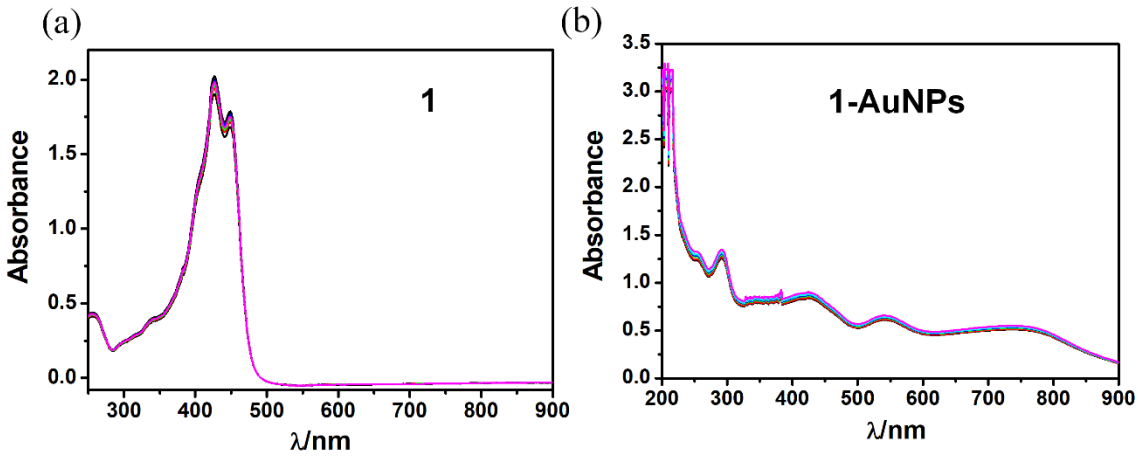

Figure S19: (a)UV-visible spectral traces **1** in 2% DMSO-H_2O (100 μM) in DMEM cell media on exposure to the red light (30W), (b) UV-visible spectral traces **1-AuNPs** in 2% DMSO-H_2O in DMEM cell media (100 μg/mL) in red light (30W) at 298 K.

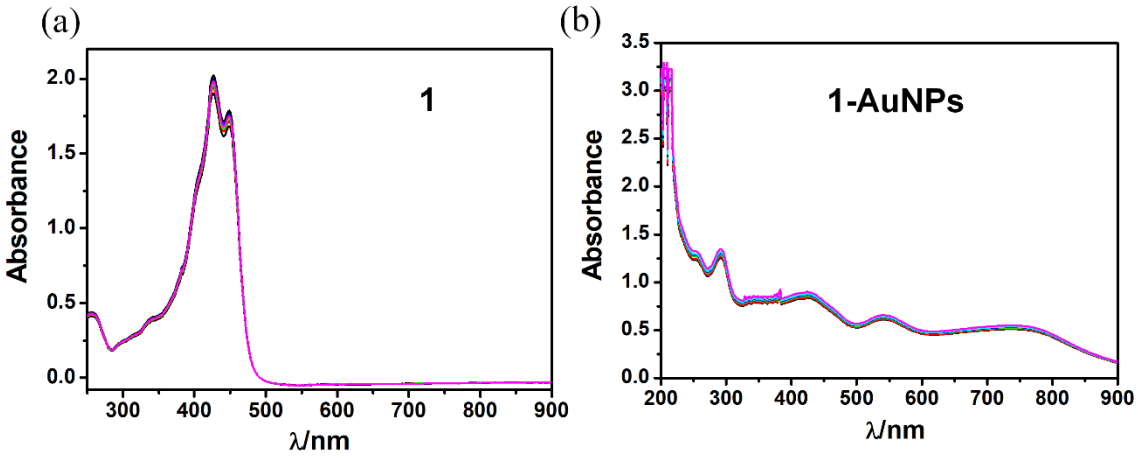

Figure S20: (a)UV-visible spectral traces **1** in 2% DMSO-H_2O in DMEM cell media (100 μM) on exposure to the dark; (b) UV-visible spectral traces **1-AuNPs** in 2% DMSO-H_2O in DMEM cell media (100 μg/mL) in dark at 298 K.

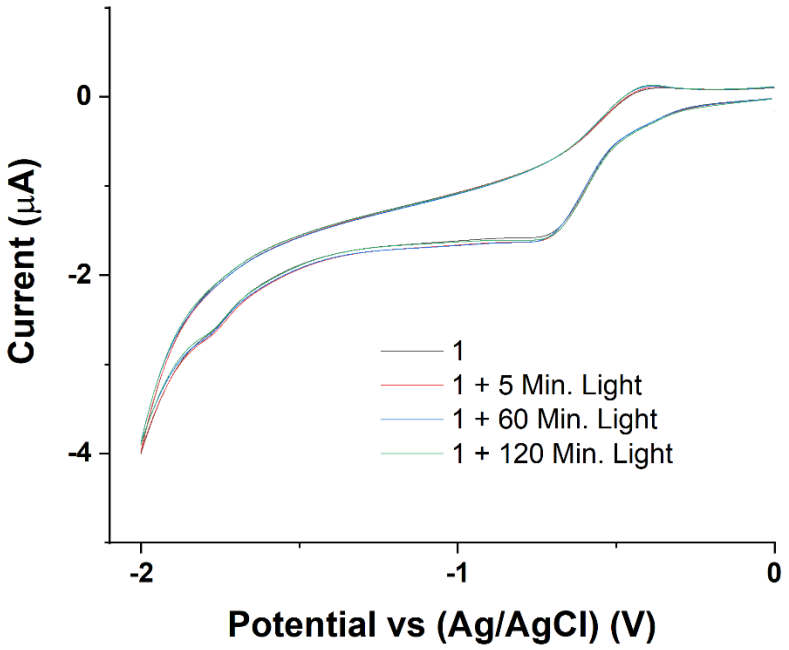

Figure S21: Cyclic Voltammogram of Complex **1 (**1mM in DMF) in presence of light is done using Glassy Carbon electrode as the working electrode, Ag/AgCl electrode as reference electrode and Pt electrode as counter electrode and TBAP (Tetrabutaylammonium perchlorate) 0.1 M as supporting electrolyte.

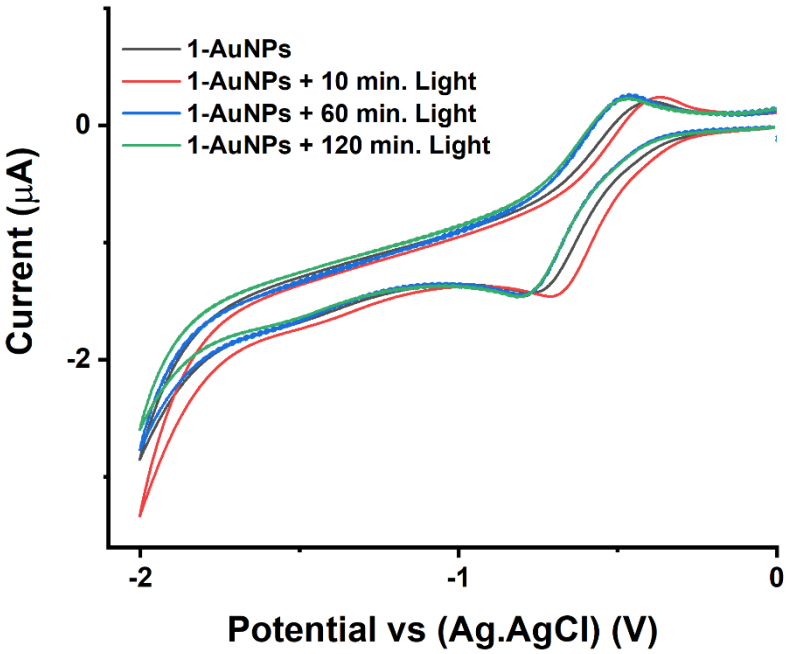

Figure S22: Cyclic Voltammogram of Complex **1-AuNPs (**100 µg in DMF) in presence of light is done using Glassy Carbon electrode as the working electrode, Ag/AgCl electrode as reference

electrode and Pt electrode as counter electrode and TBAP (Tetrabutaylammonium perchlorate) 0.1 M as supporting electrolyte.

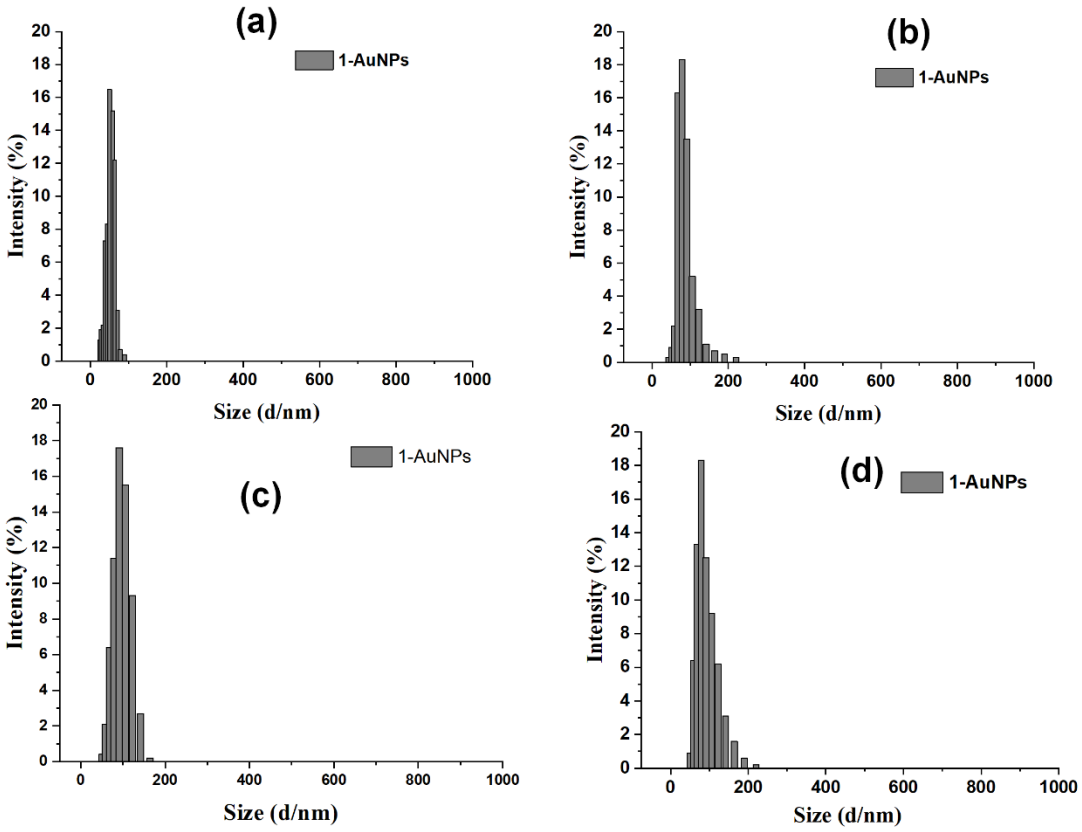

Figure S23: The particle size analysis by time to time (a) 1 day; (b) 30 days; (c) 60 days; (d) 90 days.

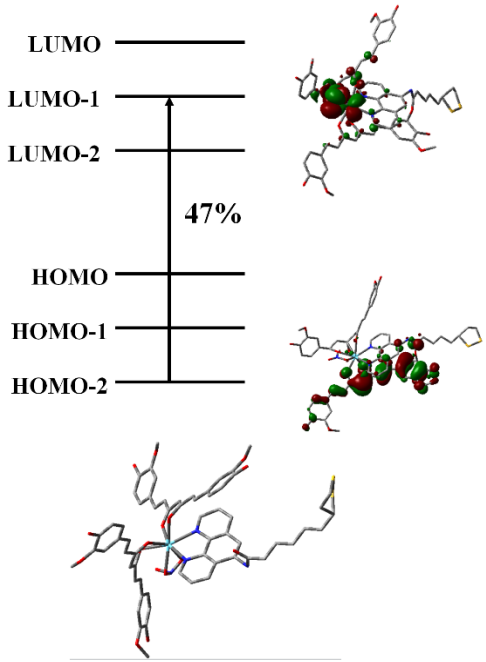

Figure S24: Selected electronic transitions predicted on the basis of TD-DFT Calculations. Calculated at TD-DFT//B3LYP/6-31G(d,p)/LanL2DZ level in gas phase with Gaussian 09W.

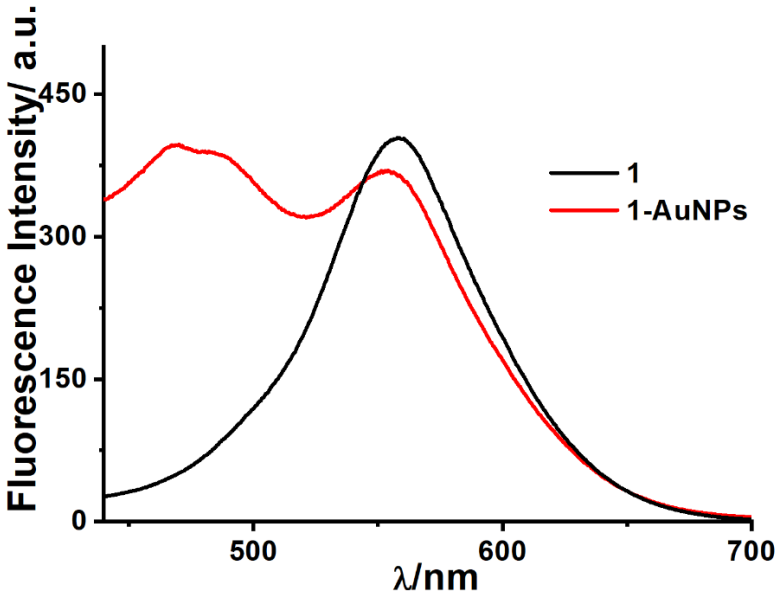

Figure S25: Emission spectra of complex (**1**) (100 μM), and **1-AuNPs** (100 μg/ml) in 2% DMSO-H_2O in DMEM cell media at 298 K (λ_{ex}, 450 nm).

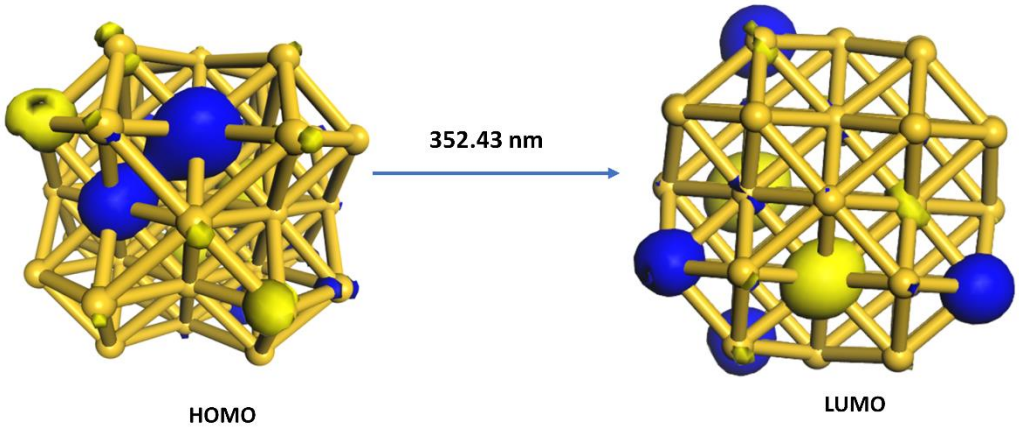

Figure S26: HOMO and LUMO stereographs of the **AuNPs** from DFT calculation at material studio software.

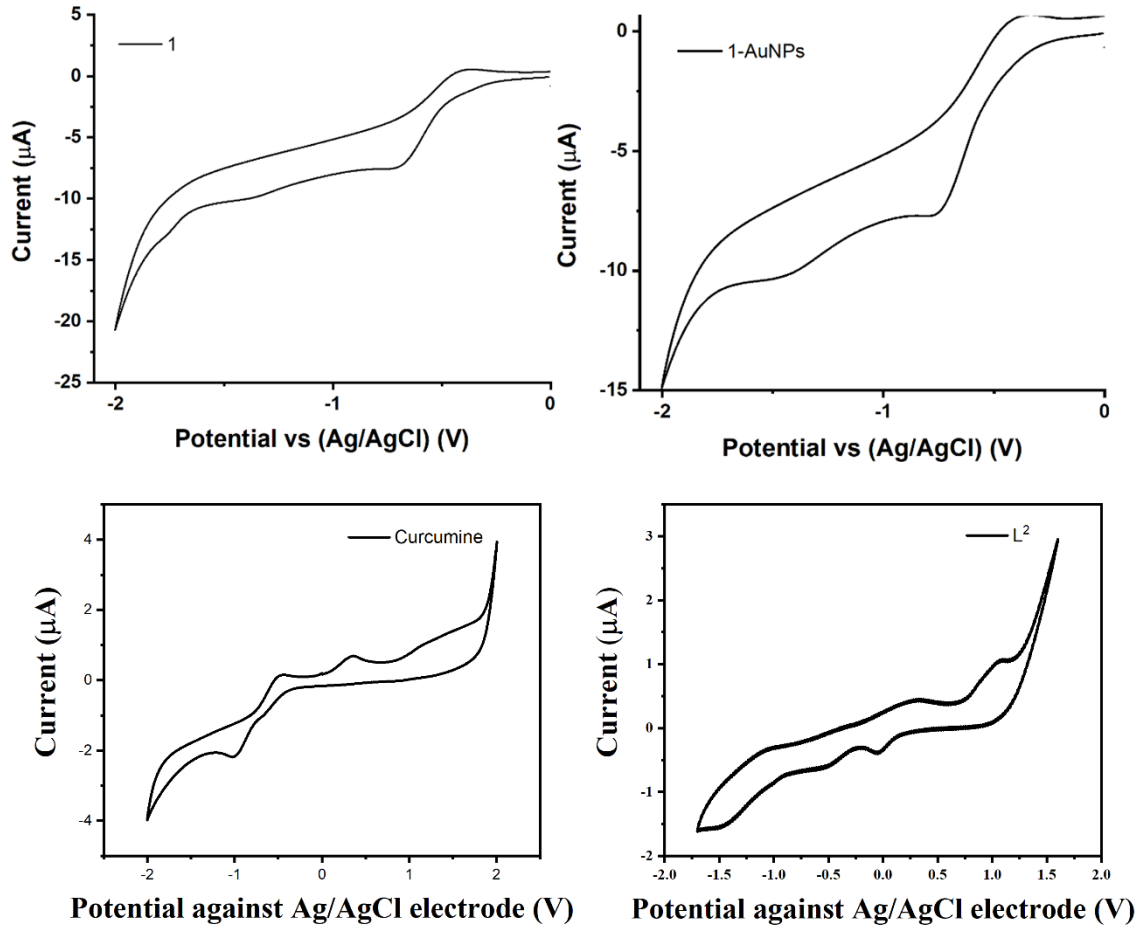

Figure S27: Cyclic Voltammogram of Ligands (L^2, Curcumin), Complex **1 (**1mM in DMF) and **1-AuNPs (**100 µg in DMF) are done using Glassy Carbon electrode as the working electrode, Ag/AgCl electrode as reference electrode and Pt electrode as counter electrode and TBAP (Tetrabutaylammonium perchlorate) 0.1 M as supporting electrolyte.

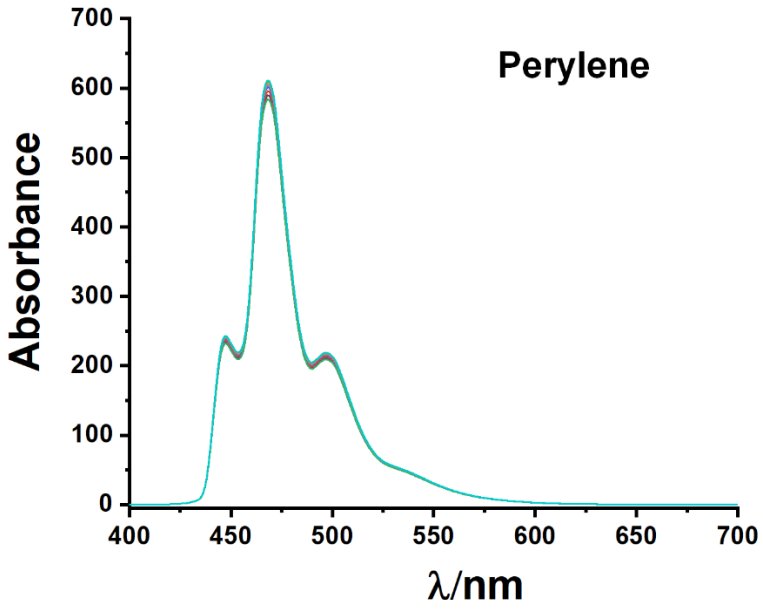

Figure S28: Up-conversion emission spectra of the Perylene after 20 min. light (Red LED, 30W) recorded in CH_3CN.

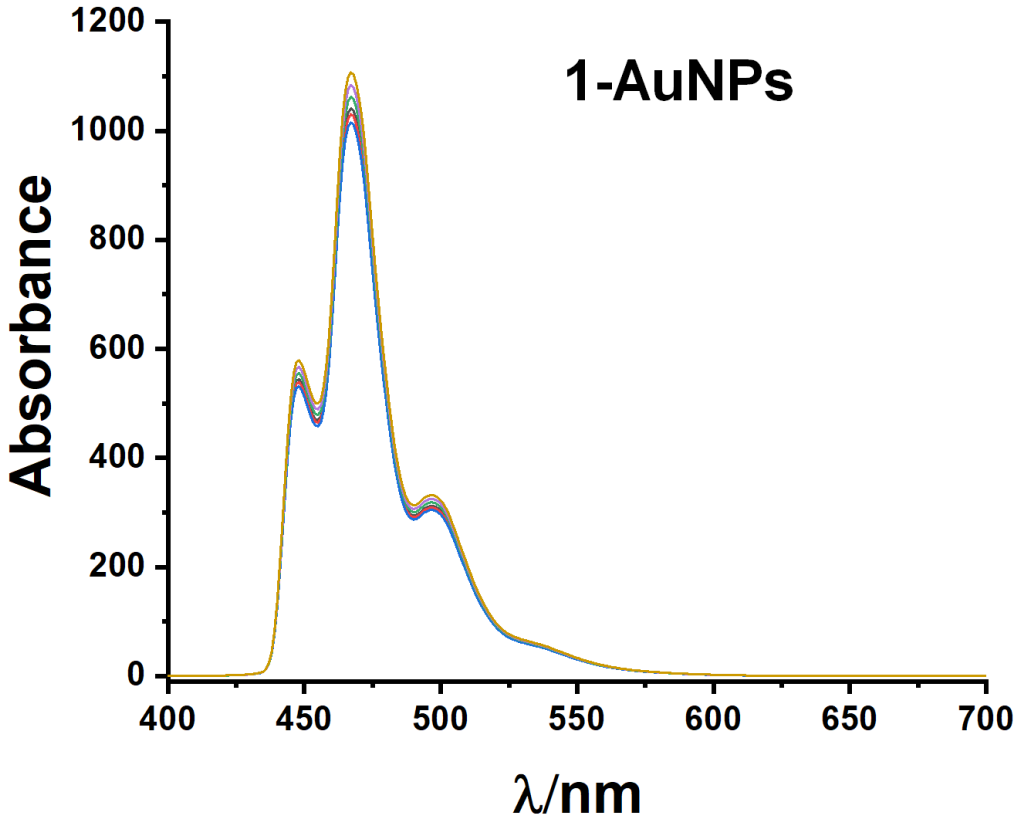

Figure S29: Up-conversion emission spectra of the 1-AuNPs and acceptor (Perylene) in dark recorded in CH_3CN.

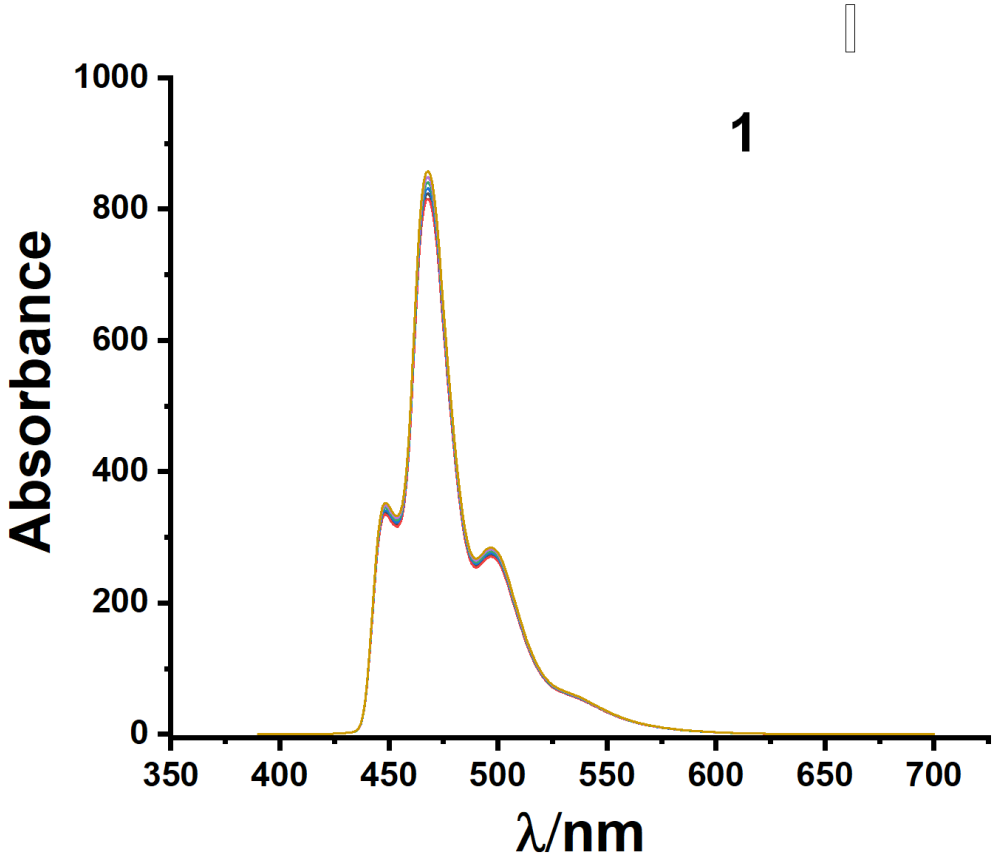

Figure S30: Up-conversion emission spectra of the complex (**1**) and acceptor (Perylene) in dark recorded in CH_3CN.

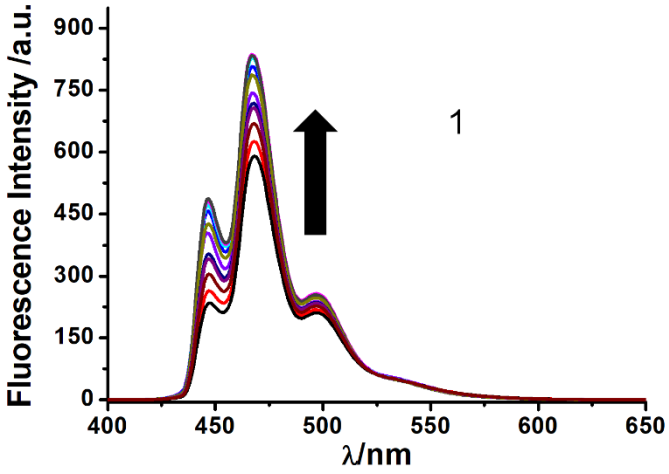

Figure S31: Up-conversion emission spectra of the complex (**1**) and acceptor (Perylene) after 20 min. light (400-700 nm) recorded in CH_3CN indicating the presence of triplet excited state in the complex; [complex] = 50 µM, [Perylene] = 250 µM (λ_{ex} = 375 nm).

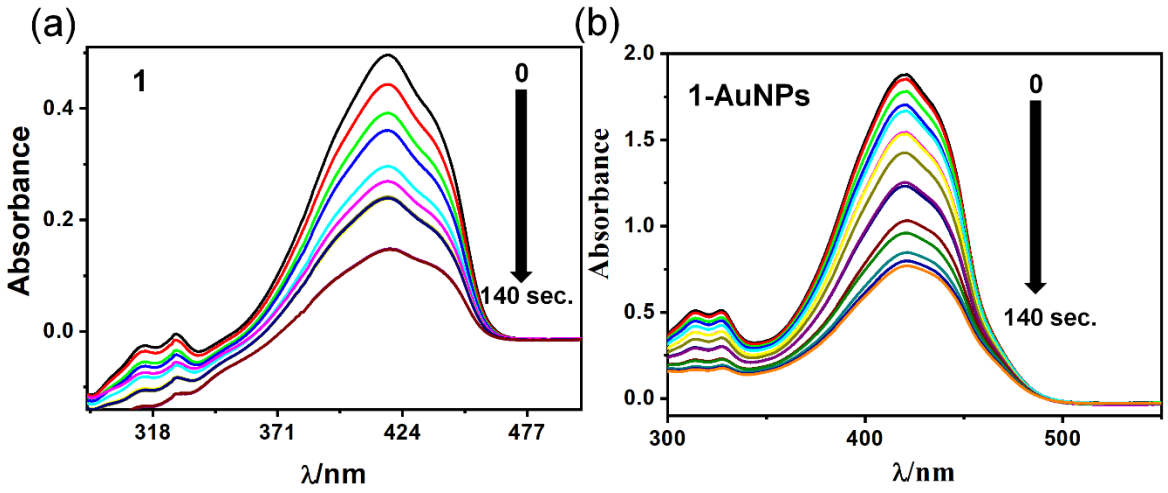

Figure S32: (a) Absorption spectral traces of diphenylisobenzofuran (DPBF) (50 µM) treated with **1** (100 µM) on exposure to red light (Red LED, 30W). (b) Absorption spectral traces of diphenylisobenzofuran (DPBF) (50 µM) treated with **1-AuNPs** (100 µg/mL) on exposure to red light (Red LED, 30W).

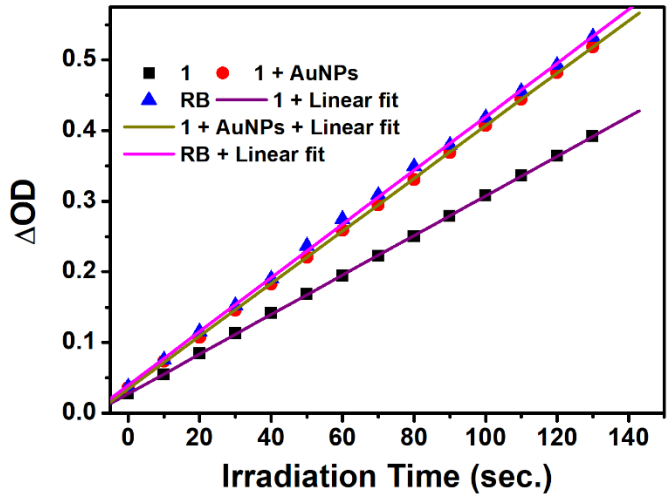

Figure S33: Singlet oxygen ($^1O_2$) quantum yield determination of the complex (**1**) (10 µM) and **1-AuNPs** (100 µg/ml) by using Rose Bengal as reference in DMSO.

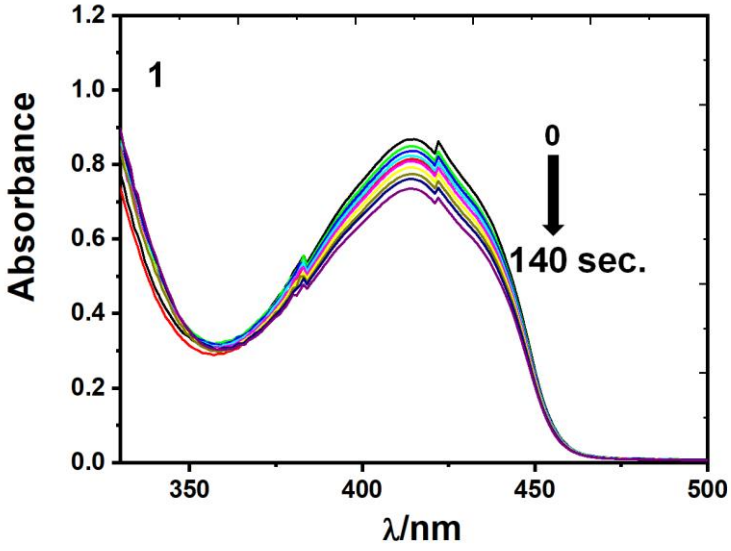

Figure S34: Absorption spectral traces of diphenylisobenzofuran (DPBF) (50 μM) treated with **1** (100 μM) in dark.

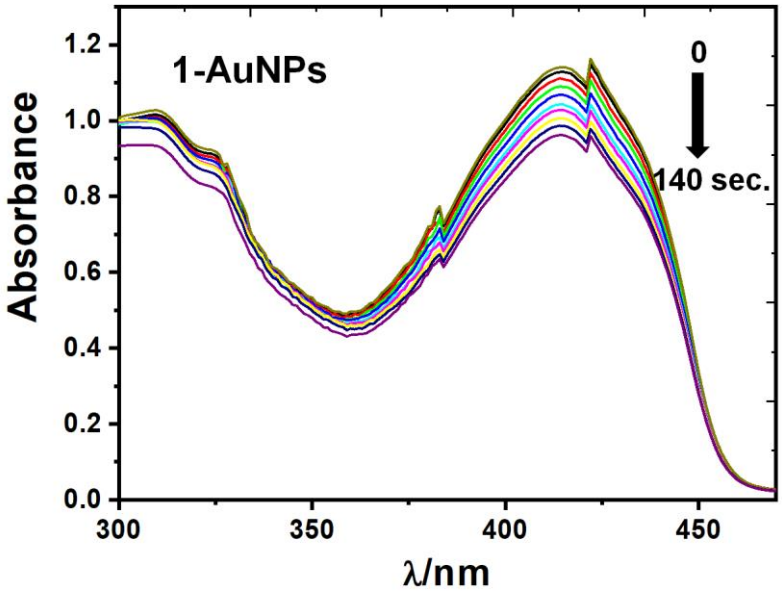

Figure S35. Absorption spectral traces of diphenylisobenzofuran (DPBF) (50 μM) treated with **1-AuNPs** (100 μg/mL) in dark.

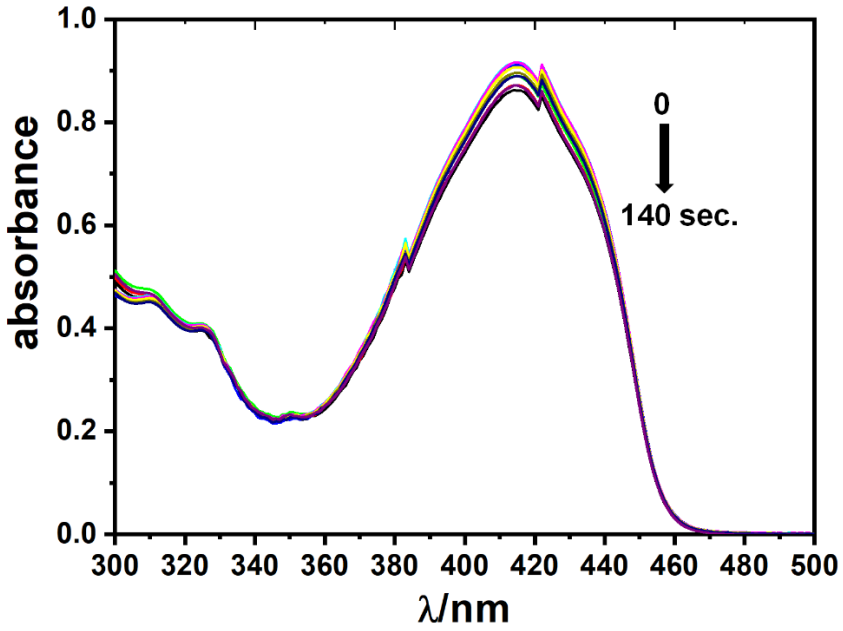

Figure S36: Absorption spectral traces of diphenylisobenzofuran (DPBF) (50 µM) alone in presence of red light (Red LED, 30W).

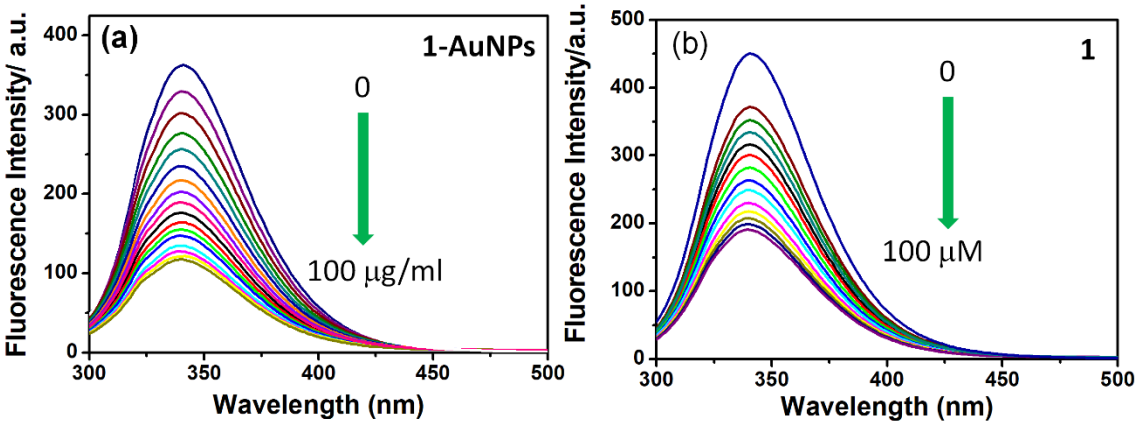

Figure S37: Fluorescence spectral traces of BSA showing the quenching effect in addition of (a) complex **1-AuNPs** and (b) 1 in Tris-HCl buffer (5 mM, pH 7.2) at 25^0c.

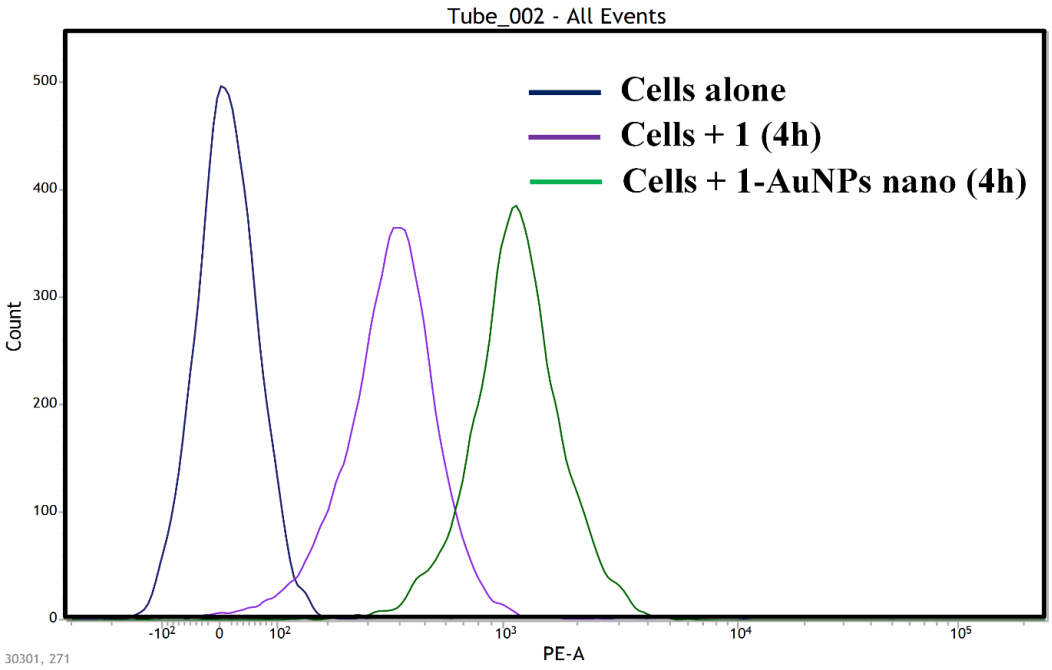

Figure S38: The FACS data from the cellular uptake study of complex (**1)** and **1-AuNPs** (12 µg) in A549 cells after 4 h incubation.

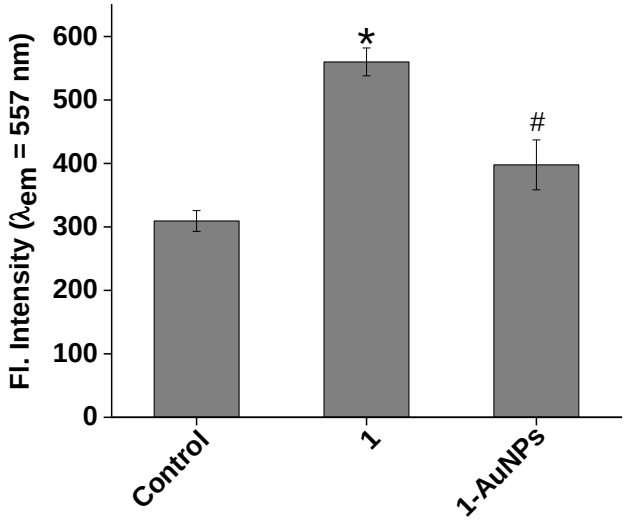

Figure S39: Cellular uptake level of complex **1** (12 µM) and **1**-AuNPs (12 µg/ml) in A549 cells after 4 h incubation is presented in terms of the mean fluorescence in tensity (MFI) monitored at 557 nm after excitation at 450 nm using multi well plate reader. The results are presented as mean ± SEM (n=4). *<0.5 as compared to control by student 't" test. #<0.05 as compared to complex 1 by student 't" test.

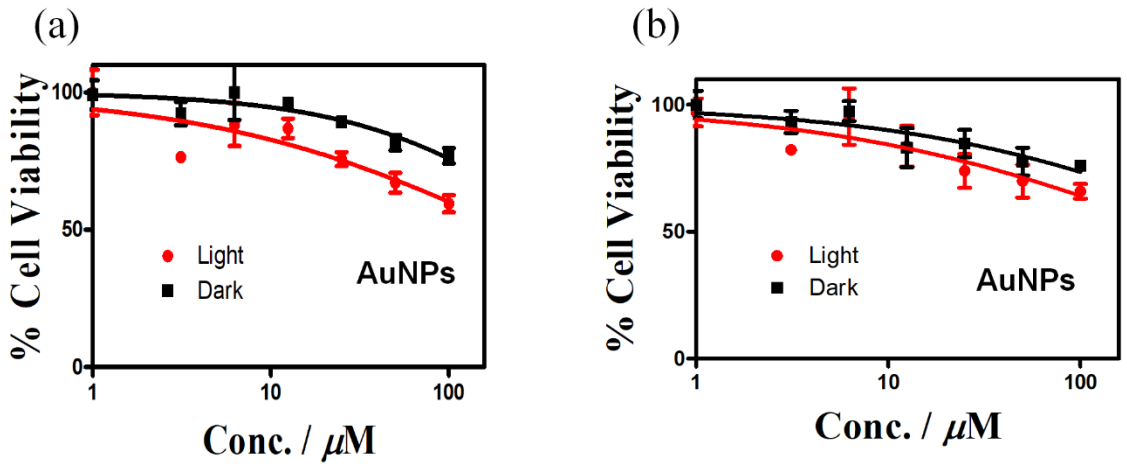

Figure S40: MTT assay plot for the complex 1 and 1-AuNPs (a) in A549; and (b) in HaCaT cells in presence of red light (600−720 nm, 30 J cm^{-2}) and dark.

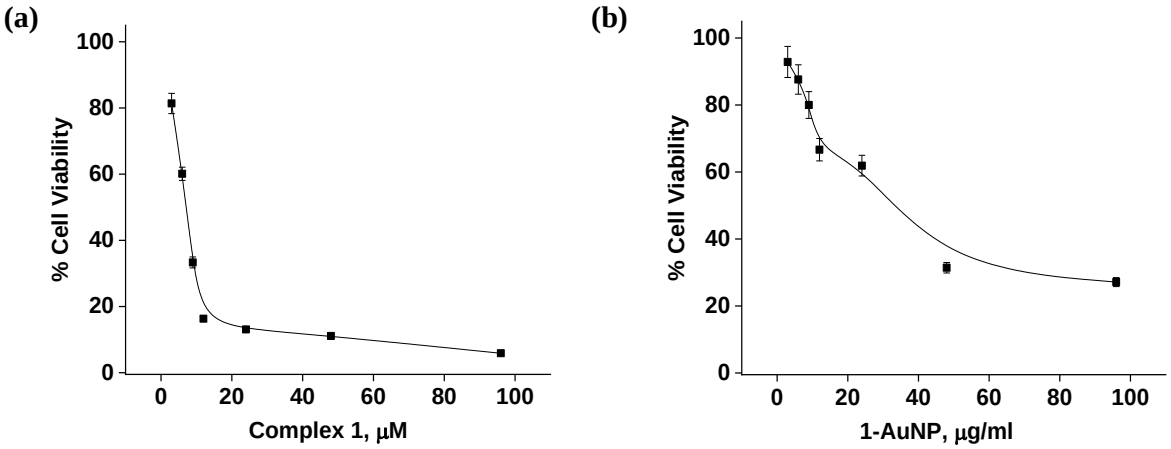

Figure S41: MTT assay plot for the (a) complex 1 (b) 1-AuNPs in WI-26VA4 cells in the presence of red light (600-720 nm,30 J cm^{-2}).

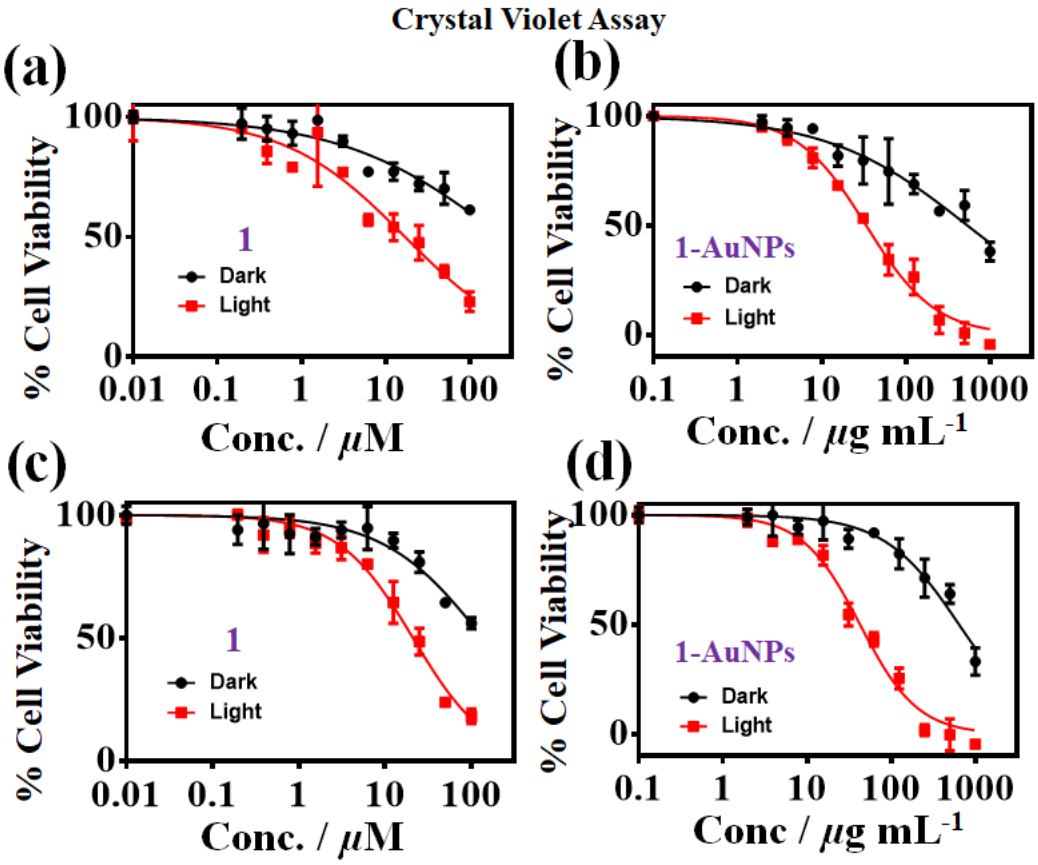

Figure S42: CVS assay plot for the complex 1 and 1-AuNPs (a) in A549; and (b) in HaCaT cells in presence of red light (600−720 nm, 30 J cm^{-2}) and dark.

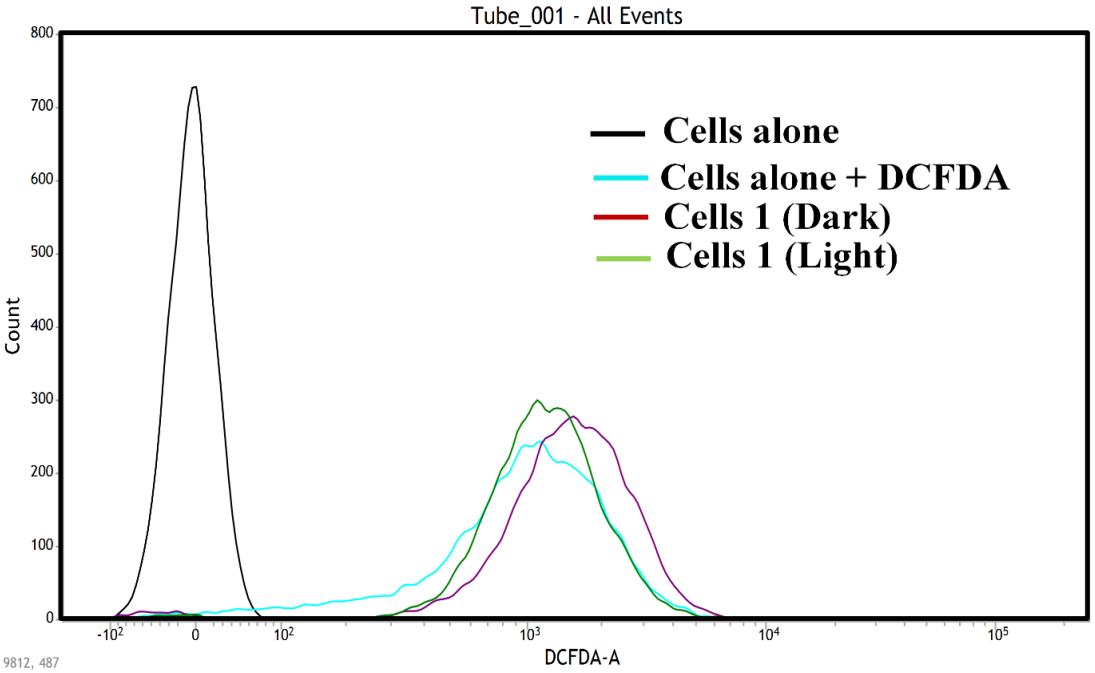

Figure S43: Fluorescence Assisted Cell Sorting (FACS) analysis for in vitro ROS generation in A549 cells by photo-activated complex **1** (12 µM) using DCFDA dye. Generation of ROS was marked by the shift in fluorescence band positions compared to cells alone in A549 cells treated with complexes in dark or red light (600−720 nm, 30 J cm^{-2}), as shown by the different colour codes.

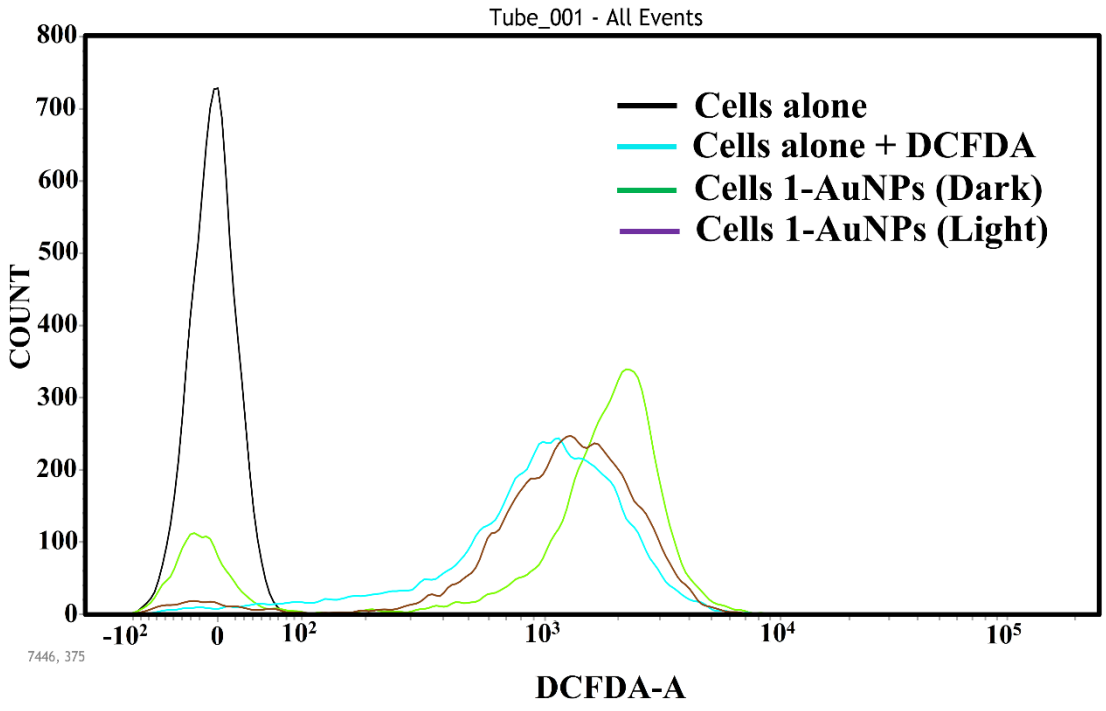

Figure S44: Fluorescence Assisted Cell Sorting (FACS) analysis for in vitro ROS generation in A549 cells by photo-activated **1-AuNPs** (12 µg/ml) using DCFDA dye. Generation of ROS was marked by the shift in fluorescence band positions compared to cells alone in A549 cells treated with complexes in dark or red light (600−720 nm, 30 J cm^{-2}), as shown by the different colour codes.

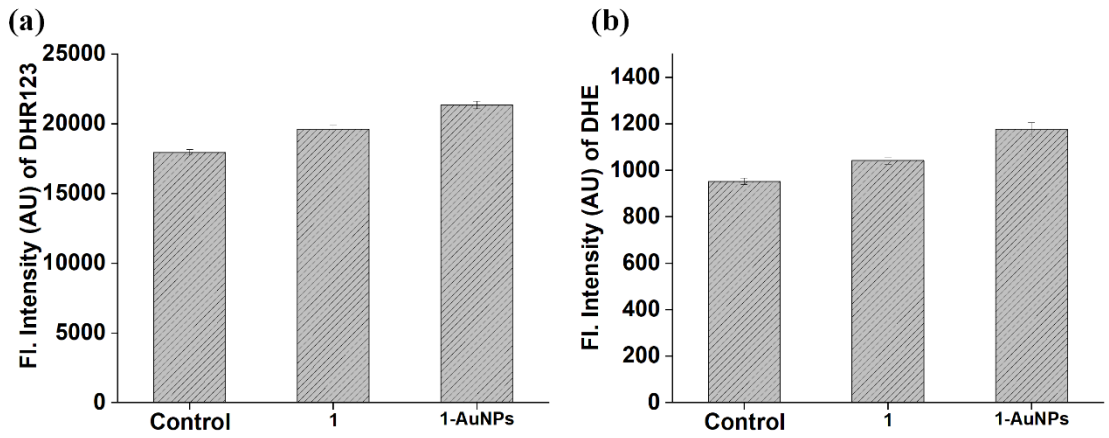

Figure S45: (a) Intracellular ROS level in A549 cell following treatment with complex **1** (12 µM) and **1**-AuNPs (12 µg/ml) under light irradiation (600-720 nm,30 J cm^{-2}). The cells were stained DHR123 (5 µM) after 30 min of light irradiation, and used for fluorescence measurement at 536 nm after excitation at 500 nm using multi well plate reader. The results are presented as mean ± SEM (n=4). (b) Intracellular ROS level in A549 cell following treatment with complex **1** (12 µM) and **1**-AuNPs (12 µg/ml) under light irradiation (600-720 nm,30 J cm^{-2}). The cells were stained DHE (5 µM) after 30 min of light irradiation, and used for fluorescence measurement at 582 nm after excitation at 500 nm using multi well plate reader. The results are presented as mean ± SEM (n=4).

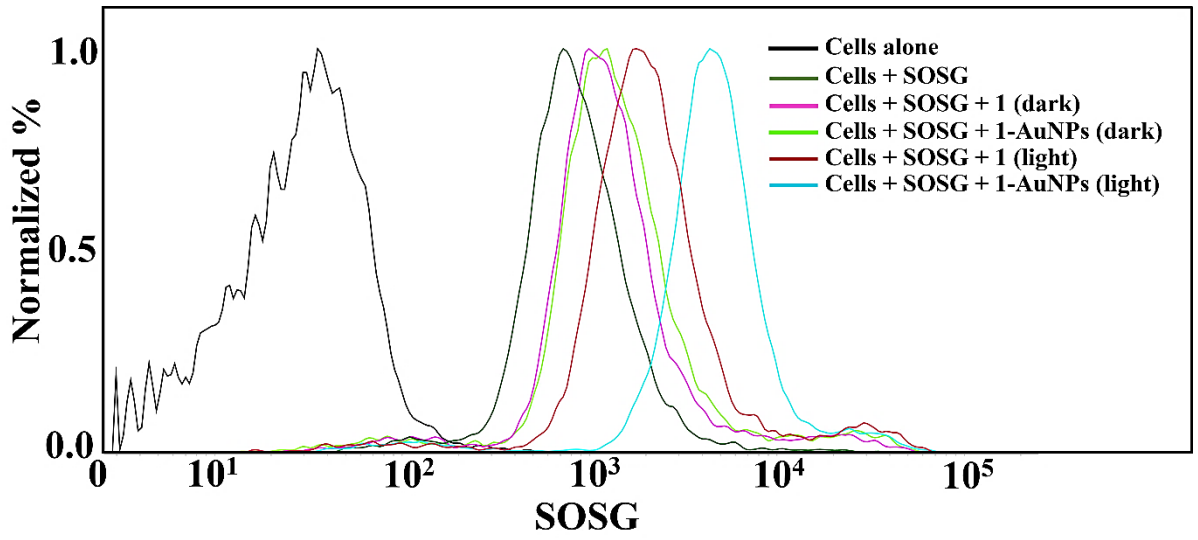

Figure S46: Fluorescence Assisted Cell Sorting (FACS) analysis for in vitro ROS generation in A549 cells by photo-activated complex **1** (12 µM) and **1**-AuNPs (12 µg/ml) using Singlet Oxygen Sensor

Green (SOSG) probe. Generation of ROS was marked by the shift in fluorescence band positions compared to cells alone in A549 cells treated with complexes in dark or red light (600−720 nm, 30 J cm^{-2}), as shown by the different colour codes.

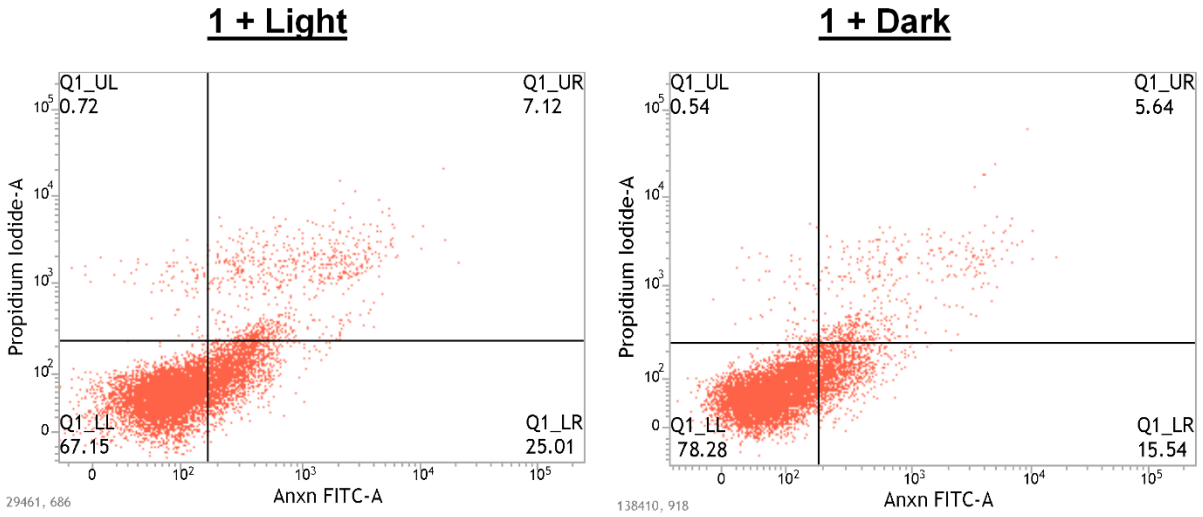

Figure S47: Annexin V-FITC/PI coupled to flow cytometry analysis showing apoptosis induced by complex **1** (12 μM) in the presence of dark and red light (600–720 nm, 30 J cm^{-2}).

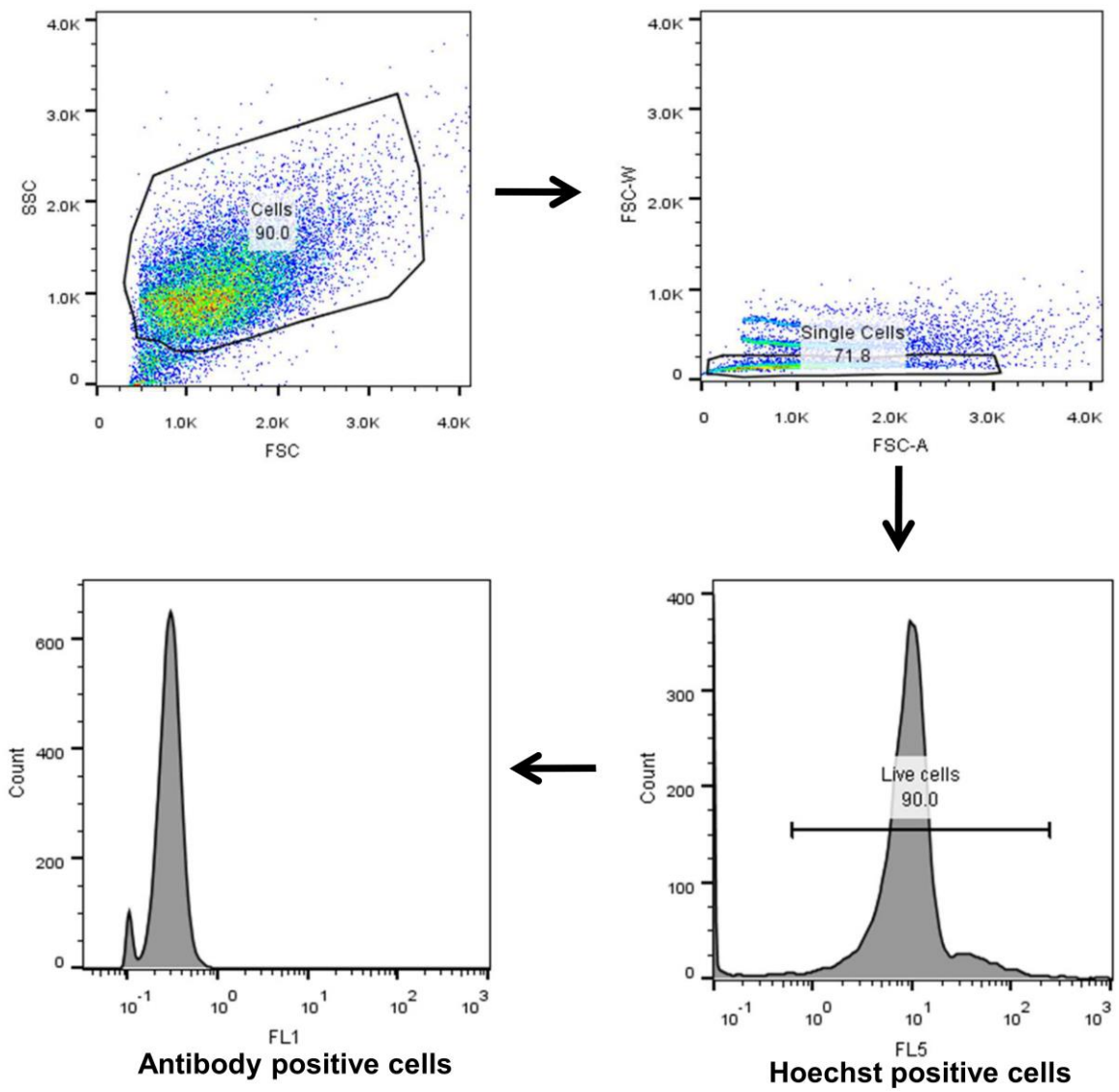

Figure S48: Representative sematic of the gating strategy followed for the flow cytometric analysis of the expression levels of BAX, Bcl-2 and cleaved caspase-3 is presented.